

**Identification and characterization of effector candidate protein
genes of *Rhizoctonia solani* AG-1 IA, a causal agent of sheath
blight disease using *Brachypodium distachyon***

September 2020

Sobhy Salama Hussein Abdelsalam

Graduate School of Environmental and Life Science

(Doctor's Course)

OKAYAMA UNIVERSITY, JAPAN

**Identification and characterization of effector candidate protein
genes of *Rhizoctonia solani* AG-1 IA, a causal agent of sheath
blight disease using *Brachypodium distachyon***

A Thesis

**Submitted to the Graduate School of Environmental and Life
Science in partial fulfillment of the requirements for the degree of
Doctor of Philosophy in agriculture**

Division Agricultural and Life Science

Okayama University

By

Sobhy Salama Hussein Abdelsalam

September 2020

TABLE OF CONTENTS

| Contents | Page |
|---|------|
| Acknowledgments | 5 |
| Abstract of the thesis | 6 |
| References | 9 |
| List of Figures | 10 |
| List of Tables | 11 |
| Chapter 1 | |
| General introduction | |
| General introduction | |
| 1.1 The global impact of plant pathogens on crops | 13 |
| 1.2 The safeguard system in plants against pathogens | 13 |
| 1.3 How pathogens attack their host plant | 14 |
| 1.4 The pathogen, <i>Rhizoctonia solani</i> | 17 |
| 1.5 Classification and host range | 17 |
| 1.6 Sheath blight, a significant disease of rice | 18 |
| 1.7 <i>Brachypodium distachyon</i> , a model monocotyledonous plant | 19 |
| 1.8 The aim of this study and the general outline of the thesis | 19 |
| References | 20 |
| Chapter 2 | |
| Development and validation of an inoculation method for early detection of <i>Rhizoctonia solani</i> on <i>Brachypodium distachyon</i> | |
| Abstract | 25 |
| Introduction | 26 |
| Materials and methods | |
| Plant and fungal materials | 28 |
| RNA-seq analysis | 28 |
| Inoculation test | 28 |
| Detection of fungal biomass and in-planta differentially expressed genes | 29 |
| Results | |
| Modification of <i>R. solani</i> inoculation method on <i>B. distachyon</i> detached leaves | 30 |
| Evaluation of the inoculation system with characterized genes | 34 |
| Discussion | 36 |
| References | 38 |
| Chapter 3 | |
| Identification of effector protein genes from <i>Rhizoctonia solani</i> using the publicly available genome sequence and bioinformatics tools. | |
| Abstract | 41 |
| Introduction | 42 |
| Materials and methods | |
| Identification of <i>RsSEPGs</i> | 44 |
| Results | |
| Surveillance of secretory effector-like protein genes (<i>RsSEPGs</i>) in <i>R. solani</i> | 45 |
| Discussion | 47 |
| References | 48 |

| Contents (continued) | Page |
|--|------|
| Chapter 4 | |
| Calibration of gene model of <i>RsSEPGs</i> with RNA-seq data | |
| Abstract | 51 |
| Introduction | 52 |
| Materials and methods | |
| RNA-seq analysis from <i>R. solani</i> | 53 |
| Results | |
| Correction of <i>RsSEPGs</i> list by calibration of gene model with RNA-sequencing data | 54 |
| Discussion | 56 |
| References | 57 |
| Chapter 5 | |
| Expression profiles and functional analysis of <i>RsSEPGs</i> during infection | |
| Abstract | 60 |
| Introduction | 61 |
| Materials and Methods | |
| Plant and fungal materials | 64 |
| RNA-seq analysis | 64 |
| Inoculation test | 64 |
| Gene expression analysis | 64 |
| z-scaling and k-means clustering of expression profiles of <i>RsSEPGs</i> | 64 |
| Plasmid construction of <i>RsSEPGs</i> expressed in the necrotrophic stage | 64 |
| Transient Expression of <i>RsSEPGs</i> in <i>B. distachyon</i> , <i>A. thaliana</i> and <i>N. benthamiana</i> | 65 |
| Semi-quantitative RT-PCR | 65 |
| Results | |
| Analysis of transcriptions of <i>RsSEPGs</i> during infection on <i>B. distachyon</i> | 66 |
| k-means clustering of gene expression patterns of <i>RsSEPGs</i> | 69 |
| Comparison of the expression profiles of <i>RsSEPGs</i> with the previously characterized <i>R. solani</i> secretory genes on rice | 73 |
| Transient expression of <i>RsSEPGs</i> expressed in the necrotrophic stage of infection | 76 |
| Discussion | 79 |
| References | 82 |
| Appendices | 85 |

ACKNOWLEDGEMENTS

I would like to express my deepest gratitude to my main supervisor Professor Yoshiteru NOUTOSHI, for giving me the opportunity to pursue my studies in his laboratory and for his patience, motivation, valuable advice, guidance, and supervision. His review of the manuscript is greatly appreciated.

I wish to express sincere thanks to my co-supervisors Professor Kazuhiro TOYODA and Professor Yuki ICHINOSE, their comments, and advice through this work are much appreciated and acknowledged.

I would also extend my thanks to Professor Hidenori MATSUI and Professor Mikihiro YAMAMOTO for their comments and suggestions to improve my studies.

I want to acknowledge current and former colleagues from the Laboratory of Plant Pathology and Genetic Engineering and Egyptian friends for their help to cope with lab work and daily activities in Okayama.

Financial support from the Egypt Japan education partnership program (EJEP) is greatly acknowledged and appreciated. My thanks also extended to the Egyptian embassy staff for their continued help and support.

Last but not least, I want to express my deepest gratitude to my family and my wife for their endless support and encouragement during my work.

Abstract of the thesis

Rhizoctonia solani is a necrotrophic plant pathogen widely distributed in soil (Ogashi 1987). Pathogenic isolates of *R. solani* AG-1 IA causes rice sheath blight disease which accounts for a 50% yield loss (Lee and Rush 1983, Zheng *et al.* 2013). In general, disease-resistance cultivars are the most effective practice for controlling plant disease, but resistant cultivar to sheath blight is not available in rice. Therefore, fungicides are the only current practical measures for the protection of rice from this disease. However, the emergence of some fungicide-resistant *R. solani* isolates were reported in the US; consequently, integrated approaches including alternative methods are desired in the world. For this aim, understanding of pathogen infection mechanisms is needed, but it remains unclear. Infection strategy varies across plant pathogens. They are classified into biotrophs, necrotrophs, and hemibiotrophs based on their nutrient intake methods. Biotrophic pathogens thrive on living plant cells but necrotrophs obtain nutrients from killed host tissues (Glazebrook 2005). Biotrophic pathogenic fungi secrete particular proteins, so-called effector proteins, to avoid host sensing mechanisms and suppress plant defense responses. Some of them work at apoplastic space to block host-derived lytic enzymes and some of them are translocated into host cells to target host immunity components. On the contrary, necrotrophs kill plant tissues by toxins and cell wall lytic enzymes to obtain nutrients. *R. solani* is considered as a necrotrophic pathogen because it induces necrosis quickly upon inoculation.

Model experimental plants can be useful tools to study plant-pathogen interaction. *Brachypodium distachyon* is a small grass closely related to cereals (tribe Triticeae). It has a short life cycle and can easily grow in laboratories. In our laboratory, *R. solani* was shown to infect *B. distachyon* and it can be a model pathosystem for molecular studies on sheath blight disease (Kouzai *et al.*, 2018). This previous study also demonstrated that two *B. distachyon* accessions were resistant to *R. solani* AG-1 IA, a causal agent of rice sheath blight, by inducing a typical disease resistance response which is mainly employed by plants to cope with infection by biotrophic pathogens (Kouzai *et al.* 2018). These results suggest that *R. solani* has an early short biotrophic phase in which small secreted effector proteins are used. Hence, this study aims to identify the candidate secreted effector proteins in *R. solani* using the model plant *B. distachyon* and characterize their functions.

The critical step to identify effector protein is gene expression analysis. An extensive time series RNA-sequencing analyses during infection of *R. solani* on rice were reported previously (Zheng *et al.* 2013, Yamamoto *et al.* 2019). In these studies, expressions of 234

potential secreted protein genes, which include possible effector candidates, were detected in the inoculated rice tissues sampled at 10–72 hours post-inoculation (hpi). However, it is possible that these studies could not fully detect the potential effector genes' expression, especially at early infection timing, because the amount of fungus derived RNAs in the infected plant sample is so small. To overcome this issue, the inoculation method was improved in this study. Firstly, the number of agar plugs, as an inoculum, on single-detached *B. distachyon* leaf was increased from 1 to 3. Secondly, the agar plugs were separated from leaves by insertion of the parafilm sheet. This method increased the pathogen population inside leaves as well as infection synchronicity by avoiding the direct infections from the agar inoculum and detecting the infection events from newly extended aerial hyphae from the inoculum.

By using this method, the inoculated leaves were harvested at 4, 6, 10, 16, 24, and 32 hpi, and RNAs were extracted for cDNA synthesis and subsequent qRT-PCR. Then the fungus derived RNAs in the samples were detected using 18S rRNA marker gene. The fungal RNAs could be detected from 6 hpi, and its level massively increased during infection up to 32 hpi. Thus, this method enabled us to monitor the fungal RNA expression at 6 hpi reproducibly. Hence, this modified method is expected to provide a better platform for the detection of gene expression of *R. solani* genes at the early infection stage.

Next, the expression analysis of four carbohydrate-active enzymes (CAZymes) genes, previously detected by Zheng *et al.*, 2013, confirmed that their expression patterns were consistent on rice and *Brachypodium*. These results suggest that *R. solani* uses a similar infection strategy on both rice and *Brachypodium* and support the value of the usability of *R. solani* -*B. distachyon* model pathosystem for sheath blight disease.

The potential effector protein genes of *R. solani* were then extracted from the publicly available genome sequence using bioinformatics tools which can predict secreted proteins, effectors, and non-membrane proteins. In total, 88 genes were identified as a candidate and they were named *RsSEPGs* stands for *R. solani* secretory effector-like protein genes. Gene structures (exon-intron prediction) of *RsSEPGs* were validated by comparing their RNA-sequence data obtained from *R. solani* hyphae grown on PDA medium. As a result, it was revealed that the publicly available prediction data of most *RsSEPGs* were incorrect. Based on this calibration, some *RsSEPGs* were out of secretion proteins due to alterations of initial codon positions leading to a lack of signal peptides. This suggests the limitation and difficulties of computational prediction of gene models for small secretory proteins. Throughout this careful validation process, 68 out of 88 *RsSEPGs* were finally selected which meet the criteria for effector.

In our infection system, the expression of 52 but not 9 *RsSEPGs* was successfully detected by qRT-PCR. They displayed variable and phase-specific expression patterns during the time course. K-means clustering algorithm was used to divide *RsSEPGs* by their expression patterns and they were classified into 6 clusters. The clusters 1 to 3 comprise 23 *RsSEPGs* whose expression levels mainly peaked before 24 hpi, and the remaining clusters 4 to 6 contain 29 *RsSEPGs* whose highest expression levels were at 24 or 32 hpi. In this platform, the disease symptoms appeared at 24 hpi, therefore, genes found in clusters 1–3 and 4–6 are expected to be involved in biotrophic and necrotrophic interactions, respectively. By using this approach, the expression patterns of 22 *RsSEPGs* were newly characterized in this study.

These results opened new avenues to study if *R. solani* employs effector proteins in its infection. Further functional studies such as protein physiological properties or target identification can clarify the infection process of *R. solani* on the molecular level.

References

- Glazebrook, J. Contrasting mechanisms of defense against biotrophic and necrotrophic pathogens. *Annu. Rev. Phytopathol.* 43, 205–227 (2005).
- Kouzai, Y. *et al.* Salicylic acid-dependent immunity contributes to resistance against *Rhizoctonia solani*, a necrotrophic fungal agent of sheath blight, in rice and *Brachypodium distachyon*. *New Phytol.* 217, 771–783 (2018).
- Lee, F.N & Rush, M.C. Rice sheath blight: A major rice disease. *Plant Dis.* 67, 829–832 (1983).
- Ogoshi, A. Ecology and pathogenicity of anastomosis and intraspecific groups of *Rhizoctonia solani* Kuhn. *Annu. Rev. Phytopathol.* 25, 125–143 (1987).
- Yamamoto, N. *et al.* Integrative transcriptome analysis discloses the molecular basis of a heterogeneous fungal phytopathogen complex, *Rhizoctonia solani* AG-1 subgroups. *Sci. Rep.* 9, 19626 (2019).
- Zheng, A. *et al.* The evolution and pathogenic mechanisms of the rice sheath blight pathogen. *Nat. Commun.* 4, 1424 (2013).

List of Figures

| Figures description | Page |
|---|------|
| Figure 1. The illustration depicts the outcomes of plant-pathogen interaction. | 14 |
| Figure 2. The improved inoculation method of <i>Rhizoctonia solani</i> on <i>Brachypodium distachyon</i> . | 32 |
| Figure 3. Evaluation of the inoculation method using <i>R. solani</i> genes whose expression patterns during inoculation on rice plants have been characterized. | 35 |
| Figure 4. The pipeline used for effector prediction from the annotated protein sequences of <i>R. solani</i> . | 44 |
| Figure 5. The protein organization of the potential secretory effector-like protein genes (<i>RsSEPGs</i>). | 45 |
| Figure 6. An example of reads alignment view showing different data depending on the zoom level displayed by IGV. | 53 |
| Figure 7. Expression profiles of <i>RsSEPGs</i> during the infection of <i>Rhizoctonia solani</i> on detached leaves of <i>Brachypodium distachyon</i> which showed different expression patterns in two independent experiments. | 68 |
| Figure 8. Expression dynamics and of <i>RsSEPGs</i> during infection on <i>Brachypodium distachyon</i> and their clustering with expression patterns. | 70 |
| Figure 9. Expression profiles of <i>RsSEPGs</i> during inoculation of <i>Rhizoctonia solani</i> on detached leaves of <i>Brachypodium distachyon</i> . | 71 |
| Figure 10. Expression profiles of <i>RsSEPGs</i> during inoculation of <i>Rhizoctonia solani</i> on detached leaves of <i>Brachypodium distachyon</i> . | 72 |
| Figure 11. The Agro-infiltration and expression of <i>RsSEPGs</i> in <i>Nicotiana benthamiana</i> . | 78 |

List of Tables

| Tables description | Page |
|--|-------|
| Table 1. Primers used in this study to validate the inoculation test | 31 |
| Table 2. Summary of RNA-sequencing analysis of <i>Rhizoctonia solani</i> growth stage on <i>R. solani</i> infection stages on detached leaves of <i>Brachypodium distachyon</i> Bd21 and Bd3-1 | 33 |
| Table 3. The potential predicted <i>Rhizoctonia solani</i> secretory effector-like protein genes (<i>RsSEPGs</i>) | 46 |
| Table 4. Summary of RNA-sequencing analysis of <i>Rhizoctonia solani</i> growth stage on PDA after 72 hpi | 54 |
| Table 5. Validation of the gene structures of predicted <i>Rhizoctonia solani</i> AG1-IA secretory effector protein genes (<i>RsSEPGs</i>) | 55 |
| Table 6. Gene ID and primer list used for qRT-PCR | 67 |
| Table 7. <i>Rhizoctonia solani</i> AG-1 IA secretory effector protein genes (<i>RsSEPGs</i>) with their expressions during infection and agar medium | 74-75 |
| Table 8. Primers used for plasmid construction for transient expression of <i>RsSEPGs</i> expressed in the necrotrophic stage of <i>R. solani</i> infection. | 77 |

Chapter 1

General introduction

General introduction

1.1 The global impact of plant pathogens on crops

Agriculture production is a limiting factor for maintaining global food security, which is the most pressing issue worldwide (Stefanis 2014, Sundström *et al.* 2014). However, the crops are hampered by environmental changes, desertification, water scarcity, and the spread of diseases and pests of plants and animals; hence, food security is greatly challenged (UNESC 2007, Suzuki *et al.* 2014). Plants are sessile and continuously exposed to a plethora of pathogens such as fungi, bacteria, nematodes, and parasitic plants (Agrios 2005, Freeman and Beattie 2008, Suzuki *et al.* 2014). Besides, viruses are possibly transmitted to plants during feeding by insects or other means of transmission (Whitfield *et al.* 2015). Plant diseases could rapidly spread under certain circumstances and become an epidemic, thereby causing severe losses. Plant disease epidemics have occurred in several agricultural communities and, therefore, food shortage has developed (Ojiambo *et al.* 2017). The well-known example is the Irish potato famine in the 1940s caused by the oomycete *Phytophthora infestans* that causes the late blight disease in potato (Ojiambo *et al.* 2017). The corn crop in the USA was destroyed in some areas owing to the spread of *Cochliobolus heterostrophus*, the causal agent of southern corn leaf blight, in 1970–1971 (Strange and Scott 2005). The rice brown spot disease caused by *Cochliobolus miyabeanus* led to a significant food shortage and a severe famine happened in the Bengal in 1943 (Padmanabhan 1973). *Rhizoctonia solani*, which caused sheath blight disease in rice, could spread rapidly in favorable conditions and causes up to 50% loss in rice yield (Lee and Ruch 1983, Zheng *et al.* 2013). Given that rice is a common food commodity for most of the world's population, many people are directly affected by rice sheath blight disease. Therefore, it is evident that plant pathogens are considered a major threat to global food security.

1.2 The safeguard system in plants against pathogens

Plants are equipped with a robust defense system, including passive/non-specific protection barriers provided by physical and chemical defenses (Dangl and Jones 2001). Additionally, plants could activate rapid active/specific defenses, including chemical (ROS production and antimicrobial compounds) and physical defenses (cell wall reinforcement) (Bacete *et al.* 2018). Generally, plant resistance is categorized into two main components of the plant immune system. The first one is using transmembrane recognition receptors to recognize microbe/pathogen-associated molecular patterns (MAMPs or PAMPs) and it

activates defense responses so-called PAMP or MAMPs-triggered immunity (PTI). The second one is deploying the resistance genes (*R* genes) that encode nucleotide-binding and leucine-rich repeats (NB-LRR) proteins. NB-LRRs, in turn, recognize diverse effector proteins derived from pathogens and it activates defense responses named effector-triggered immunity (ETI) (Figure1) (Jones and Dangl 2006).

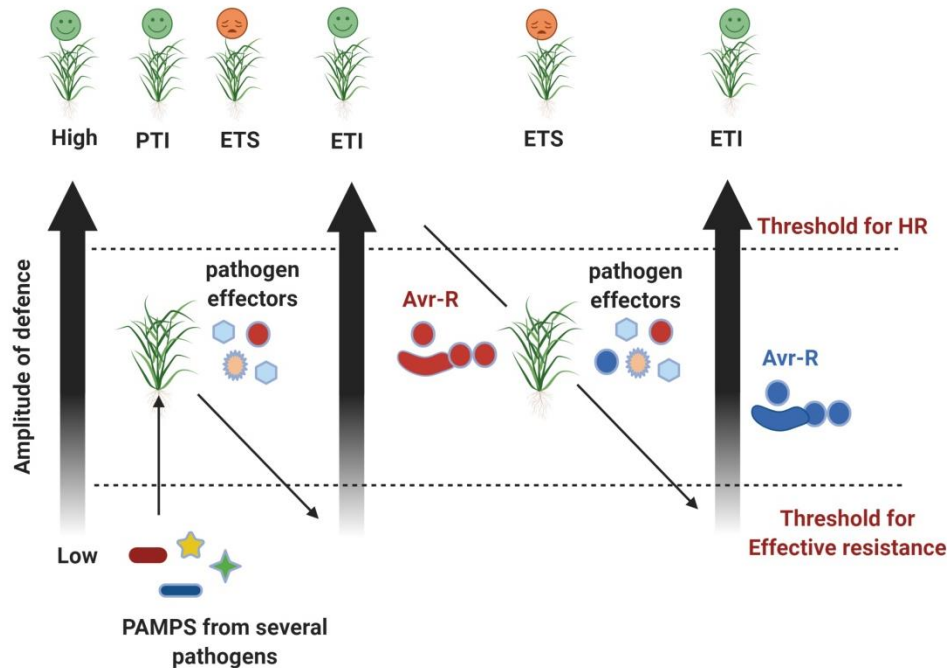


Figure 1. The illustration depicts the outcomes of plant-pathogen interaction; primarily, plants perceive MAMPS or PAMPS and therefore trigger PTI. Secreted effectors enable pathogens to interfere with PTI and thus resulting in effector-triggered susceptibility (EST). In some cases, plants could recognize the secreted effector *via* NB-LRR protein and triggered ETI. Because of the rapid evolution of effector genes, plant pathogens could gain or lose an effector/s to suppress ETI. (Designed by BioRender)

1.3 How pathogens attack their host plant

Phytopathogens have ever-evolving pathogenicity to defeat plant defenses and colonize plant tissues for adequate growth and reproduction. Therefore, successful pathogens can breach the plant defenses and obtain nutrients from plants in a different manner based on their lifestyle (Rodriguez-Moreno *et al.* 2108, Sánchez-Vallet *et al.* 2018). Plant pathogens are classified into biotrophic, hemibiotrophic, and necrotrophic based on their nutrition uptake strategies. Biotrophs boom on the living tissue, while necrotrophs gain the nutrients by killing plant tissues. The hemibiotrophs have an intermediate lifestyle between biotrophs and necrotrophs.

Necrotrophs are thought to pass through a short period of biotrophy at the onset of infection followed by the necrotrophic stage (Glazebrook *et al.* 2005, Rodriguez-Moreno *et al.* 2107). According to their lifestyle, the mode of pathogenesis also varied among plant pathogens. Suppression of plant immunity is an essential infection strategy to establish biotrophic infection. In this regard, the secretion of effector protein is commonly employed, and they ultimately facilitate invasion and tissue manipulation by suppressing plant immunity (Glazebrook *et al.* 2005, S´anchez-Vallet *et al.* 2018). In the necrotrophic infection, toxins and cell wall degrading enzymes are mainly used to rapidly kill plant tissues to uptake nutritional contents from the dead cells (Gebrie 2016).

Pathogens have evolved an arsenal of weapons to penetrate and break down plant defense barriers. The mechanical force such as turgor pressure generated from the apical hyphal growth or the appressorium is a useful tool to facilitate infection (Agrios 2005, Malinovsky *et al.* 2014, Bastmeyer *et al.* 2002, Ryder and Talbot 2015, Krishnan *et al.* 2018). Production of a wide range of bioactive chemical molecules such as enzymes, proteins, peptides, secondary metabolites, effectors, phytohormones and toxins, and nucleic acids are also crucial chemical tools for the successful invasion of host plants (Agrios 2005, Chanclud and Morel 2016, Chanclud *et al.* 2016, Vincent *et al.* 2020). Cell wall-degrading enzymes have been reported to be widely used by pathogens to depolymerize the cell wall's main component, such as cellulose, hemicellulose, and pectin (Walton 1994, Kubicek *et al.* 2014). The emerging of next-generation sequencing technology has propelled the determination of the whole-genome sequences of the number of phytopathogen genomes. In combination with functional analysis, the number of pathogen's genes has been substantially identified which are crucial for virulence (Mohanta and Bae 2015, Kubicek *et al.* 2014). Recent genomic studies have shown great diversity in cell wall degrading enzymes secreted by plant pathogens. It is more common in the necrotrophs comparing to biotrophs and hemibiotrophs (Kubicek *et al.* 2014). Most importantly, carbohydrate-active enzymes (CAZymes) were found to be crucial for pathogenicity in many fungi. Amongst 675 CAZymes genes identified from the genome of *Alternaria alternata*, several of them were differentially regulated in transcription (Ma *et al.* 2019). *R. solani* was revealed to encode diverse sets of secreted proteins and enzymes and expressions of several CAZyme genes such as glycoside hydrolase (GH) and polysaccharide lyase (PL) were detected during the interaction between *Rhizoctonia* and rice (Zhang *et al.* 2013, Yamamoto *et al.* 2019). *Fusarium graminearum*, *Fusarium virguliforme*, and *Fusarium proliferatum* also secrete many proteins, including cell wall-degrading enzymes, which are vital for pathogenicity (Rampitsch *et al.* 2013, Chang *et al.* 2016, Li *et al.* 2019). Bacteria and

nematodes similarly secrete cell wall-degrading enzymes during infection to gain nutrients from plant tissues (Bauters *et al.* 2014, Niemi *et al.* 2017). For example, the genome sequence of the necrotrophic pathogen of potato, *Pectobacterium carotovorum* strain SCC1, possesses several cell wall degrading enzymes. These enzymes include pectate lyases, polygalacturonases, and oligogalacturonate lyase. Also, other cellulases, rhamnogalacturonate lyase, pectin methylesterases, and pectin acetylerases, and some protease were identified in this bacterium (Niemi *et al.* 2017). The rice nematode *Hirschmanniella oryzae* and other fungi produce a hemicellulose-degrading enzyme β -mannanase that belongs to glycoside hydrolase 5 (GH5) and GH26 CAZyme families (Takahashi *et al.* 2013, Bauters *et al.* 2014, Soni *et al.* 2017).

Phytopathogens widely deploy secreted proteins so-called effectors which are implicated in suppressing plant defense systems (Abramovich *et al.* 2003). Effectors are small, cysteine-rich, and secreted proteins usually expressed *in planta* to facilitate infection (Sperschneider *et al.* 2016). Several effectors, regarded as core effectors, were found to be conserved among phytopathogens and have a significant contribution to its virulence (Irieda *et al.* 2019). For instance, NIS1 is one of the core effector proteins found in *Colletotrichum* spp and it suppresses PAMP-induced hypersensitive response and oxidative burst in *Nicotiana benthamiana* (Irieda *et al.* 2019). In *C. fructicola*, a conserved secreted effector protein CfEC92 can promote early appressorial penetration to apple leaves by suppressing PTI responses (Shang *et al.* 2020). The LysM-containing effectors are involved in scavenging some PAMPs to hide from sensing by the host plants. The LysM effector RsLysM from *R. solani* and SIP1 from *Magnaporthe oryzae* also bind to chitin fragments released from the fungal cell wall during infection. They compete with PRR-type chitin sensor proteins and eventually suppress the chitin-triggered PTI response (Zhang and Xu 2014, Dolfors *et al.* 2019).

Toxins and secondary metabolites produced by plant pathogens, especially necrotrophs, are crucial strategies for plant tissue invasion (Walton 1996, Agrios 2005). Pathogen-produced toxins have lethal effects on plant cells and help to use cell contents as a nutrient source. Some toxins kill plants specifically or non-specifically by affecting the plasma membrane's integrity, leading to leakage of the cell's main components. Additionally, some of them could target organelles such as chloroplasts and mitochondria and suppress the activities of some essential enzymes hence disrupt the biochemical processes necessary for the synthesis of crucial metabolites (Walton 1996, Agrios 2005, Möbius and Hertweck 2009, Tsuge *et al.* 2012, Rauwane *et al.* 2020). Several toxins produced by the necrotrophic pathogen *Fusarium* spp,

including fumonisins, trichothecenes, and zearalenone have negatively affected crop production (Rauwane *et al.* 2020). A toxin named Ptr ToxA from *Pyrenophora tritici-repentis* was found to induce necrosis and chlorosis on wheat leaves when its purified protein was infiltrated into leaves (Tuori *et al.* 2000). Victorin is a toxin produced by *Cochliobolus victoriae*, the causal agent of Victoria blight disease in oats, and it has an essential role in pathogenicity and disease progression. (Lorang *et al.* 2007). In *Alternaria alternata*, the causal agent of brown spot disease in citrus, production of host-selective toxin ACT is critical for its pathogenic capability (Ma *et al.* 2019). Therefore, studying the mechanisms of infection and pathogenicity and virulence factors is important to uncover a more comprehensive view of the virulence mechanisms of phytopathogens.

1.4 The pathogen, *Rhizoctonia solani*

R. solani is a soil-borne plant pathogen with a broad host range (Anderson 1982, Ajayi-Oyetunde *et al.* 2018). *Rhizoctonia* is a species complex categorized into 14 anastomosis groups (AG) with great diversity in cultural morphology, growth characteristics, and pathogenicity (Anderson 1982, Zheng *et al.* 2013, Ajayi-Oyetunde *et al.* 2018). *R. solani* belongs to Basidiomycota and its average genome size is around 46.48 Mb (Mohanta and Bae 2015). The genome sequences of many isolates of *R. solani* has been released so far, and they are varied in their sizes. The genome size of *R. solani* AG-1 IA, the causal agent of sheath blight disease, is estimated to be 36.94 Mb in size (Zheng *et al.* 2013, Nadarajah *et al.* 2017). *R. solani* AG-1 IA encodes large sets of genes related to pathogenicity and virulence that is thought to contribute to its wide distribution and host range (Zheng *et al.* 2013).

1.5 Classification and host range

R. solani exists as thread-like growth or as a hard-dark mass of hyphae named sclerotia on plants or its debris in the soil; this fungus belongs to:

Kingdom: Fungi

Division: Basidiomycota

Class: Agaricomycetes

Order: Cantharellales

Family: Ceratobasidiaceae

Genus: *Rhizoctonia*

Species: *R. solani*

The teleomorph (*Thanatephorus cucumeris*) stage rarely exists in nature, but the anamorph stage (*R. solani*) is the most ubiquitous (Ajayi-Oyetunde *et al.* 2018, Uppala and Zhou 2018). *Rhizoctonia* was reported to infect the essential food crops worldwide, such as cereals, cotton, sugar beet, potato, field crops, turfgrasses, ornamentals, fruit trees, and forest trees (Anderson 1982, Ajayi-Oyetunde *et al.* 2018). Based on the infected host, *Rhizoctonia* induces variable disease symptoms of which seed decay, damping-off, root rot, sheath blight, black scarf, and stem canker (Ajayi-Oyetunde *et al.* 2018). There are many reports regarding the identification of *R. solani* as a causal agent of various crop diseases. Certain AG groups are frequently found in a specific plant species and the AG groups are thought to be related to the host specificity. However, this is still unclear.

1.6 Sheath blight, a significant disease of rice

Rice sheath blight is a disease caused by *R. solani* and is considered a second dangerous disease to the rice blast (Lee and Rush 1983). This disease can rapidly spread in favorable conditions in rice fields and causes necrosis and collapse. Sheath blight disease can also affect the grain and reduces its quality. Losses caused by this disease could reach 50% in conducive environments. Usually, the life cycle of *R. solani* starts with mycelial growth from the overwintering sclerotia and they attach to rice seedlings or plants. Then the mycelia move upward along sheaths and leaves and it causes tissue necrosis. Eventually, it results in damages on the sheaths, leaves, and grains. At the end of the life cycle, the fungus forms sclerotia on plant parts, debris, and soil, and they can be initial inocula for the next infection cycle (Uppala and Zhou 2018). In the rice field, it is normally co-suppressed by fungicides such as QoI inhibitors which are used for rice blast. In some cases, fungicides applicable to *R. solani* specifically are also used in a severely diseased situation. Recently, the emergence of resistance isolates against QoI has been reported in the US. Therefore, alternative approaches for disease control are desired. However, disease resistance cultivars to *R. solani* are not available in rice because all rice cultivars and wild rice strains are susceptible.

1.7 *Brachypodium distachyon*, a model monocotyledonous plant

B. distachyon is a small grass closely related to cereals (tribe Triticeae) which containing wheat and barley that are widely used food commodities (Draper *et al.* 2001). *B. distachyon* has many attractive characteristics which make it a useful model organism for broad areas of plant biological research. This plant has a standard set of biological traits as a model

plant such as short life cycle, ease of growing in the laboratory, and ease of crossing. Various experimental tools have been developed such as a diverse set of germplasm, microarray, robust protocols for transformation, and several T-DNA insertion lines (26,000 T-DNA insertion sites are available from 22,000 lines). The whole-genome sequence of *B. distachyon* is also available (Draper *et al.* 2001, Kellogg 2015). Many pathogens can infect *B. distachyon*; therefore, it has been established as a model plant to study plant-pathogen interaction. *Brachypodium* natural accessions represent varied resistance or susceptibility to several crop pathogens (Draper *et al.* 2001, Zhong *et al.* 2015 and Kouzai *et al.* 2018). *B. distachyon* was resistant to the wheat adapted pathogen *Blumeria graminis* species (Draper *et al.* 2001). More recently, Kouzai *et al.* identified three accessions resistant to *R. solani* (Kouzai *et al.* 2018, Kouzai *et al.* 2020). Six *B. distachyon* lines were found to be infected with the spot blotch pathogen *Cochliobolus sativus* with a variable degree of resistance (Zhong *et al.* 2015). Given these situations, *B. distachyon* provides a useful platform for further molecular and genetic studies of these pathogens because crops are generally large size and long lifecycle.

1.8 The aim of this study and the general outline of the thesis

This study aimed to identify and functionally characterize the candidate genes encoding effector proteins of *R. solani* (designated as *RsSEPGs* stands for *R. solani* secretory effector protein genes), which may have a role in the pathogenicity of this pathogen. In chapter 2, an inoculation method was developed and validated which enables to detect expressed genes of *R. solani* at the early infection stage in *Brachypodium distachyon*. Chapter 3 includes the identification of *RsSEPGs* from the publicly available gene annotation information of *R. solani* genome using bioinformatics tools. In chapter 4, the gene structures (Exon-Intron) of *RsSEPGs* were validated using RNA-seq data obtained from *R. solani* grown on Potato Dextrose Agar media (PDA) to select *RsSEPGs* which actually satisfy the criteria for effector proteins. Finally, in chapter 5, the expression profiles of each *RsSEPG* during infection in *B. distachyon* were analyzed. The necrosis-inducing activities of some *RsSEPGs* expressed at the later infection stage were also verified using agroinfiltration method as functional analysis.

References

- Abramovitch, R.B., Kim, Y., Chen, S., Dickman, M.B. & Martin, G.B. Pseudomonas type III effector AvrPtoB induces plant disease susceptibility by inhibition of host programmed cell death. *EMBO J.* 22, 60–69 (2003).
- Agrios, G. *Plant pathology: Fifth edition.* Plant Pathology: Fifth Edition (2004).
- Ajayi-Oyetunde, O.O. & Bradley, C.A. *Rhizoctonia solani*: taxonomy, population biology and management of rhizoctonia seedling disease of soybean. *Plant Pathol.* 67, 3–17 (2018).
- Anderson, N.A. The Genetics and pathology of *Rhizoctonia solani*. *Annu. Rev. Phytopathol.* 20, 329–347 (1982).
- Bacete, L., Melida, H., Miedes, E. & Molina, A. Plant cell wall-mediated immunity: cell wall changes trigger disease resistance responses. *Plant J.* 93, 614–636 (2018).
- Bastmeyer, M., Deising, H.B. & Bechinger, C. Force exertion in fungal infection. *Annu. Rev. Biophys. Biomol. Struct.* 31, 321–341 (2002).
- Bauters, L., Haegeman, A., Kyndt, T. & Gheysen, G. Analysis of the transcriptome of *Hirschmanniella oryzae* to explore potential survival strategies and host – nematode interactions. *Mol. Plant Pathol.* 15, 352–363 (2014).
- Chanclud, E. & Morel, J.B. Plant hormones: a fungal point of view. *Mol. Plant Pathol.* 17, 1289–1297 (2016).
- Chanclud, E. *et al.* Cytokinin Production by the rice blast fungus is a pivotal requirement for full virulence. *PLoS Pathog.* 12, 1–25 (2016).
- Chang, H.X., Yendrek, C.R., Caetano-Anolles, G. & Hartman, G.L. Genomic characterization of plant cell wall degrading enzymes and in silico analysis of xylanases and polygalacturonases of *Fusarium virguliforme*. *BMC Microbiol.* 16, 147 (2016).
- Dangl, J.L. & Jones, J.D.G. Defence responses to Infection. *Nature* 411, 826–833 (2001).
- Dörfors, F., Holmquist, L., Dixelius, C. & Tzelepis, G.A. LysM effector protein from the basidiomycete *Rhizoctonia solani* contributes to virulence through suppression of chitin-triggered immunity. *Mol. Genet. Genomics* 294, 1211–1218 (2019).
- Draper, J., Mur, L. A.J., Jenkins, G., Ghosh-Biswas G.C., Bablak P., Hasterok R. & Routledge, A. P. M. *Brachypodium distachyon*. A new model system for functional genomics in grasses. *Plant Physiol.* 127, 1539–1555 (2001).
- Freeman, B.C. & Beattie, G.A. An overview of plant defenses against pathogens and herbivores *The Plant Health Instructor* (2008) doi:10.1094/PHI-I-2008-0226-01.
- Gebrie, S.A. Biotrophic fungi infection and plant defense mechanism. *J. Plant Pathol. Microbiol.* 7, 9 (2016).

- Glazebrook, J. Contrasting mechanisms of defense against biotrophic and necrotrophic pathogens. *Annu. Rev. Phytopathol.* 43, 205–227 (2005).
- Irieda, H. *et al.* Conserved fungal effector suppresses PAMP-triggered immunity by targeting plant immune kinases. *Proc. Natl. Acad. Sci. U. S. A.* 116, 496–505 (2019).
- Jones, J.D.G. & Dangl J.L. The plant immune system. *Nature* 444, 323–329 (2006).
- Kellogg, E.A. *Brachypodium distachyon* as a genetic model system. *Annu. Rev. Genet.* 49, 1–20 (2015).
- Kouzai, Y. *et al.* Salicylic acid-dependent immunity contributes to resistance against *Rhizoctonia solani*, a necrotrophic fungal agent of sheath blight, in rice and *Brachypodium distachyon*. *New Phytol.* 217, 771–783 (2018).
- Krishnan, P. *et al.* Transposable element insertions shape gene regulation and melanin production in a fungal pathogen of wheat. *BMC Biol.* 16, 78 (2018).
- Kubicek, C.P., Starr, T.L. & Glass, N.L. Plant cell wall-degrading enzymes and their secretion in plant-pathogenic fungi. *Annu. Rev. Phytopathol.* 52, 427–451 (2014).
- Lee, F.N & Rush, M.C. Rice sheath blight: A major rice disease. *Plant Disease* 67, 829–832 (1983).
- Li, T. *et al.* Secretome profiling reveals virulence-associated proteins of *Fusarium proliferatum* during Interaction with Banana Fruit. *Biomolecules.* 9, 246 (2019).
- Lorang, J.M., Sweat, T.A. & Wolpert, T.J. Plant disease susceptibility conferred by a ‘resistance’ gene. *Proc. Natl. Acad. Sci. U. S. A.* 104, 14861–14866 (2007).
- Ma, H. *et al.* Cell-wall-degrading enzymes required for virulence in the host selective toxin-producing necrotroph *Alternaria alternata* of citrus. *Front. Microbiol.* 10, 2514 (2019).
- Malinovsky, F.G., Fangel, J.U. & Willats, W.G.T. The role of the cell wall in plant immunity. *Front. Plant Sci.* 5, 178 (2014).
- Möbius, N. & Hertweck, C. Fungal phytotoxins as mediators of virulence. *Curr. Opin. Plant Biol.* 12, 390–398 (2009).
- Mohanta, T.K. & Bae, H. The diversity of fungal genome. *Biol. Proced. Online* 17, 8 (2015).
- Nadarajah, K., Razali N.M., Cheah, B.H., Sahrana, N.S., Ismail, I., Tathode M. & Bankarc, K. Draft genome sequence of *Rhizoctonia solani* anastomosis group 1 subgroup 1A strain 1802/ KB isolated from rice. *Genome Announc* 5, e01188-17 (2017).
- Niemi, O. *et al.* Genome sequence of the model plant pathogen *Pectobacterium carotovorum* SCC1. *Stand. Genomic Sci.* 12, 87 (2017).
- Ojiambo, P.S., Yuen, J., Van Den Bosch, F. & Madden, L.V. Epidemiology: Past, present, and future impacts on understanding disease dynamics and improving plant disease

- management — A summary of focus issue articles. *Phytopathology* 107, 1092–1094 (2017).
- Padmanabhan, S.Y. The great bengal famine. *Annu. Rev. Phytopathol.* 11, 11–24 (1973).
- UNESCO. Africa review report on drought and desertification. Fifth Meet. Africa Comm. Sustain. Dev. (ACSD-5). Addis Ababa 22-25 Oct. 2007 71 (2007).
- Rampitsch, C., Day, J., Subramaniam, R. & Walkowiak, S. Comparative secretome analysis of *Fusarium graminearum* and two of its non-pathogenic mutants upon deoxynivalenol induction in vitro. *Proteomics* 13, 1913–1921 (2013)
- Rauwane, M.E. *et al.* Pathogenicity and virulence factors of *Fusarium graminearum* including factors discovered using next generation sequencing technologies and proteomics. *Microorganisms* 8, 305 (2020).
- Rodriguez-Moreno, L., Ebert, M.K., Bolton, M.D. & Thomma, B.P.H.J. Tools of the crook-infection strategies of fungal plant pathogens. *Plant J.* 93, 664–674 (2018).
- Ryder, L.S. & Talbot, N.J. Regulation of appressorium development in pathogenic fungi. *Curr. Opin. Plant Biol.* 26, 8–13 (2015).
- Sánchez-Vallet, A. *et al.* The genome biology of effector gene evolution in filamentous plant pathogens. *Annu. Rev. Phytopathol.* 56, 21–40 (2018).
- Shang, S. *et al.* A novel effector CfEC92 of *Colletotrichum fructicola* contributes to glomerella leaf spot virulence by suppressing plant defences at the early infection phase. *Mol. Plant Pathol.* 21, 936–950 (2020).
- Soni, H., Rawat, H.K., Ahirwar, S. & Kango, N. Screening, statistical optimized production, and application of β -mannanase from some newly isolated fungi. *Eng. Life Sci.* 17, 392–401 (2017).
- Sperschneider, J. *et al.* EffectorP: Predicting fungal effector proteins from secretomes using machine learning. *New Phytol.* 210, 743–761 (2016).
- Stefanis, C. Global Food Security: An agricultural perspective. *J. Agric. Sustain.* 6, 69–87 (2014).
- Strange, R.N. & Scott, P.R. Plant Disease: A threat to global food security. *Annu. Rev. Phytopathol.* 43, 83–116 (2005).
- Sundström, J.F. *et al.* Future threats to agricultural food production posed by environmental degradation, climate change, and animal and plant diseases - a risk analysis in three economic and climate settings. *Food Secur.* 6, 201–215 (2014).
- Suzuki, N., Rivero, R.M., Shulaev, V., Blumwald, E. & Mittler, R. Abiotic and biotic stress combinations. *New Phytol.* 203, 32–43 (2014).

- Takahashi, M. *et al.* Degradation and synthesis of β -glucans by a *Magnaporthe oryzae* endotransglucosylase, a member of the glycoside hydrolase 7 family. *J. Biol. Chem.* 288, 13821–13830 (2013).
- Tsuge, T. *et al.* Host-selective toxins produced by the plant pathogenic fungus *Alternaria alternata*. *FEMS Microbiol. Rev.* 37, 44–66 (2013).
- Tuori, R.P., Wolpert, T.J. & Ciuffetti, L.M. Heterologous expression of functional Ptr ToxA. *Mol. Plant-Microbe Interact.* 13, 456–464 (2000).
- Uppala, S. & Zhou, X.-G. Rice sheath blight. *Plant Heal. Instr.* (2018) doi:10.1094/PHI-I-2018-0403-01.
- Vincent, D., Rafiqi, M. & Job, D. The multiple facets of plant–fungal interactions revealed through plant and fungal secretomics. *Front. Plant Sci.* 10, 1626 (2020).
- Walton, J.D. Deconstructing the cell wall. *Plant Physiol.* 104, 1113–1118 (1994).
- Walton, J.D. Host-selective toxins: Agents of compatibility. *Plant Cell* 8, 1723–1733 (1996).
- Whitfield, A.E., Falk, B.W. & Rotenberg, D. Insect vector-mediated transmission of plant viruses. *Virology* 479–480, 278–289 (2015).
- Yamamoto, N. *et al.* Integrative transcriptome analysis discloses the molecular basis of a heterogeneous fungal phytopathogen complex, *Rhizoctonia solani* AG-1 subgroups. *Sci. Rep.* 9, 19626 (2019).
- Zhang, S. & Xu, J.R. Effectors and effector delivery in *Magnaporthe oryzae*. *PLoS Pathog.* 10, e1003826 (2014).
- Zheng, A. *et al.* The evolution and pathogenic mechanisms of the rice sheath blight pathogen. *Nat. Commun.* 4, 1424 (2013).
- Zhong, S., Ali, S., Leng, Y., Wang, R. & Garvin, D.F. *Brachypodium distachyon*-*Cochliobolus sativus* pathosystem is a new model for studying plant-fungal interactions in cereal crops. *Phytopathology* 105, 482–489 (2015).

Chapter 2

**Development and validation of an inoculation method for early
detection of *Rhizoctonia solani* on *Brachypodium distachyon***

Abstract

Rhizoctonia solani is a necrotrophic plant pathogen of the Basidiomycota divided into 14 anastomosis group (AGs). The rice sheath blight isolates that belong to AG-1 IA cause severe damage to rice plants. In this study, a detached leaf inoculation method was developed for the early detection of *R. solani in planta* using the model plant *Brachypodium distachyon*. A previous inoculation method was improved for the early detection of fungal biomass in the infected plants. The number of inocula was increased from one to three. Also, a parafilm sheet was inserted between the inoculant and leaves to increase the synchronicity of the infection hyphae. In this condition, the fresh areal mycelia were observed on the inoculated leaves at 4 hpi and the symptom has appeared at 24 hpi, two days earlier than the previous method. Then fungal biomass in plant tissues was monitored at 2 to 32 hours post-inoculation (hpi) using a quantitative reverse transcription-polymerase chain reaction (qRT-PCR). The *18S rRNA* was used as a marker gene to trace the fungal biomass. This gene could be successfully and reproducibly detected from 6 hours after inoculation. To validate the usefulness of this inoculation system; four carbohydrate-active enzymes (CAZyme) genes and three effector protein genes which were previously characterized in rice plants were reanalyzed. The expression patterns of these genes were almost consistent in both rice and *B. distachyon*. Therefore, *R. solani* may use a similar infection strategy on both plants. More importantly, this method enables us to detect the fungal RNAs *in planta* at early time points. This advantageous will be useful for further studies to unravel the earlier expressed genes with a potential role in the pathogenicity of *R. solani*.

Introduction

Rhizoctonia solani attacks a wide range of crops and induces seed decay, seedling damping off, sheath blight, stem cankers, black scurf, and root rots (Anderson 1982, Ogoshi 1987). Sheath blight disease is one of the major constraints on rice cultivation worldwide because it conduces to considerable yield losses of up to 50% (Lee and Rush 1983). Highly resistant rice cultivars are unavailable for sheath blight (Hashiba 1984). Agrochemicals are the only practical way to suppress this disease, but caution is needed not to develop fungicide resistance (Uppala and Zhou 2018). To overcome these limitations, novel crop protection measures are strongly desired which should be developed on the molecular basis of pathogen ecology and host-pathogen interaction. However, the virulence mechanisms of *R. solani* are poorly understood. *In vivo*, *R. solani* infections have been affected by various factors (Anderson 1982, Ogoshi 1987). The limiting factors of its infection are the primary fungal load in the soil or on the plant debris and environmental factors such as humidity and temperature (Ogoshi 1987, Lakshman *et al.* 2012). *R. solani* radial growth can be affected significantly at a low-temperature environment (Mazolaa *et al.* 1996). Therefore, the optimization of an *in vitro* inoculation method for *R. solani* is a limiting factor in studying its pathogenicity.

Precise detection and quantification of the fungal biomass in the infected plants is important for both diagnosis and studying virulence mechanisms of plant pathogenic fungi (Tsui *et al.* 2001). Over the years, detection methods of plant pathogens in the infected tissue have been developed for accurate and early quantification. DNA array technology, multiplex tandem PCR, padlock probe technology with rolling circle amplification, and loop-mediated isothermal amplification (LAMP) were developed to detect fungal pathogens in the environmental samples (Tsui *et al.* 2001). Genomic rDNA-based genes were employed to quantify and detect *R. solani* in the rice tissue; qRT-PCR could detect *R. solani* in infected rice tissues before symptoms appearance (Fenille *et al.* 2003, Sayler and Yang 2007). Detached leaf assay is a widely used approach to study the pathogenicity of many fungal pathogens, whereas spore suspension or single agar inoculum is used for infection (Arraiano *et al.* 2001, Zheng *et al.* 2013, Kouzai *et al.* 2018). This method was employed by Kouzai *et al.* 2018 to study the pathogenicity of *R. solani* using the model grass plant *Brachypodium distachyon*. Also, Zheng *et al.* 2013 used the same approach to investigate the pathogenicity of *R. solani* on detached rice leaves in a time-course experiment. Light necrosis was induced by this inoculation after 32 hpi subsequently severe necrosis was observed at 72hpi.

Recent genomics and transcriptomics studies have identified a great diversity in the pathogenicity genes within the genomes of many plant pathogens. Using this method Zheng *et al.* 2013 could identify diverse sets of genes encoding secreted proteins and enzymes that are possibly involved in the pathogenicity of *R. solani*. Several CAZyme genes were identified during *Rhizoctonia*-Rice interaction. Common CAZyme gene families such as glycoside hydrolase (GH) and polysaccharide lyase (PL); additionally, effector proteins with the ability to induce necrosis were identified within the genome of *R. solani* in Rice-*Rhizoctonia* interaction using the transcriptome analysis (Zheng *et al.* 2013, Yamamoto *et al.* 2019).

Despite its simplicity and ease to perform, the detached leaf assay using a single inoculum is expected to be insufficient to detect especially early expressed genes. As most of the RNA extracted from the infected tissues is a plant origin, especially at the beginning of the infection process, consequently, it is not easy to detect the early expressed pathogenicity genes (Ghosh *et al.* 2014). In *R. solani*, spores are unavailable; therefore, synchronous infection is difficult due to the uneven growth of hyphae. In a transcriptome analysis using detached leaves, from the amenable model plant, *B. distachyon*, inoculated with a single *R. solani* agar plug, no significant read counts were detected at 8 hours post-infection (hpi). To tackle this problem, the detached leaf inoculation method was improved to increase the synchronicity of fungal hyphal growth in plant tissue. Three agar inocula instead of one were taken from 3 days old *R. solani* culture and used for a single leaf blade. A parafilm sheet was inserted between the inoculum and the detached leaf to avoid direct infection from the hypha that exists on the agar plug. These modifications are expected to increase the amount of synchronous areal hyphae penetrating plant tissue. Fungal biomass in the infected *B. distachyon* leaves was detected by tracing the fungal *18S rRNA* housekeeping gene using qRT-PCR. This marker gene was reproducibly detected earlier than the previous method. Furthermore, previously detected pathogenicity genes of *R. solani* on rice were selected and their expression was found to be consistent in both studies. Further gene expression analysis using this method will lead to the detection and identification of more pathogenicity related genes in the early infection stage.

Materials and methods

Plant and fungal materials

The *B. distachyon* accession Bd21 was obtained from the National Plant Germplasm System of USDA-ARS. Dry seeds were sterilized and germinated in a plastic Petri dish with moist filter paper (Kouzai *et al.* 2018). After 7 days, the seedlings were transferred to soil (Sakata Supermix-A; Sakata Seed, Yokohama, Japan) and grown for 2 weeks in a growth chamber with LED lights (LPH-350S; Nippon Medical & Chemical Instruments, Osaka, Japan) at 25 °C under a 16 h light/8 h dark photoperiod. The *R. solani* Japanese isolate sampled from rice symptoms of sheath blight disease (MAFF Genbank stock number MAFF305230) was obtained from NARO Genbank and cultured on potato dextrose agar plates (PDA; BD, Franklin Lakes, NJ, USA) at 23 °C for 3 to 5 days.

RNA-seq analysis

Total RNA was extracted from the detached *B. distachyon* leaves inoculated with *R. solani* at 8 hpi as described previously by Kouzai *et al.* 2018 using Nucleospin RNA plant kit (Takara Bio, Kusatsu, Japan) with three biological replicates. The quality and quantity of the extracted RNA were checked using a NanoDrop OneC (Thermo Fisher Scientific, Waltham, MA, USA) and a 2100 Bioanalyzer (Agilent, Santa Clara, CA, USA). Libraries for RNA-seq were prepared using a Truseq RNA library preparation kit (Illumina, San Diego, CA, USA) according to the manufacturer's instructions, and the prepared libraries were sequenced with HiSeq4000 (Illumina). The obtained reads were firstly mapped to the *B. distachyon* reference genome (Bdistachyon_314) retrieved from Phytozome to remove the reads derived from host plants using TopHat v2.1.1 with Bowtie v2.2.6 as its mapping tool (Langmead *et al.* 2012, Kim *et al.* 2013). Secondly, the resulted unmapped reads were then mapped to the *R. solani* genome (GCA_000334115) retrieved from EnsembleFungi after discarding single reads. The number of mapped reads of each *R. solani* gene was counted and normalized by fragments per kilobase of transcript per million mapped reads (FPKM) using Cufflks (Trapnell *et al.* 2012).

Inoculation test

The inoculation method described previously (Kouzai *et al.* 2018) was modified. The third leaves of 3 weeks old plants were detached and fixed on a wet filter paper in a Petri dish. *R. solani* sub-cultured on PDA media for 3 days and mycelial agar plugs (3 mm in diameter) were prepared with biopsy punches (BP-30F, Kai corporation, Tokyo, Japan). Three Parafilm strips (4 mm in width) (Parafilm M film, Bemis Flexible Packaging, Neenah, WI, USA) were

placed evenly on a fixed *B. distachyon* leaves then 3 agar plugs were placed on each leaf. The Petri dishes were kept in a container with clear-plastic lid append with wet papers to make humid condition and the containers were put in a growth chamber at 25 °C.

Detection of fungal biomass and *in-planta* differentially expressed genes.

Inoculated leaves were sampled on several time intervals post-inoculation (2–32-hour post-inoculation (hpi)). The areal hyphae on the sampled leaves were removed by wet-wipes with 70% ethanol and adhesive tape; subsequently, leaves were immediately frozen in liquid nitrogen and stored at -80 °C. Frozen leaf samples were crashed with 4 zirconia balls (ϕ 3 mm) using a homogenizer (MicroSmash MS-100, TOMY SEIKO, Tokyo, Japan). Total RNAs were extracted using PureLink RNA Mini Kit (Thermo Fisher Scientific) according to the manufacturer instructions. Concentration and purity of extracted RNAs were checked using DS-11 Spectrophotometer (DeNovix, Wilmington, DE, USA). cDNAs were synthesized using PrimeScript RT reagent Kit with gDNA Eraser (Takara Bio). Luna Universal qPCR Master Mix (New England Biolabs, Ipswich, MA, USA) and LightCycler 96 Real-Time PCR System (Roche, Pleasanton, CA, USA) were used for qRT-PCR analysis. All experiments were performed with 4 technical replicates and repeated 2 times as biological replicates. The expression data were normalized with *18S rRNA* gene as a reference, and then relative expression for each gene was calculated according to Applied Biosystems User Bulletin #2 (P/N 4303859). Seven genes previously detected by Zheng *et al.* 2013 in infected rice were used to evaluate the inoculation method (Table 1). Primer3, an online software tool, was used to design primers for each gene (Table 1) (Untergasser *et al.* 2012).

Results

Modification of *R. solani* inoculation method on *B. distachyon* detached leaves

We have previously developed a pathosystem using *R. solani* AG-1 IA and *B. distachyon*, an experimental monocotyledonous plant (Kouzai *et al.* 2018). To analyze the expression profile of *R. solani* virulence genes during infection, we have carried out RNA-sequencing (RNA-seq) analysis using *B. distachyon* detached leaves inoculated with a single mycelial agar plug prepared from *R. solani*-growing potato dextrose agar (PDA) medium as an inoculum (Table 2). However, the read counts derived from the fungi were so small compared with those from the host at 8 hours post-inoculation (hpi), and differentially expressed genes could not be fully identified with statistical significance. To overcome this technical limitation, we decided to improve our inoculation method as well as to use qRT-PCR for detection. Firstly, the number of inocula was increased from 1 to 3 on a single leaf blade to maximize the amount of infection hyphae in the leaf samples (Figure 2a). The synchronicity of the fungal infection stage should also severely affect the result of gene expression analysis. In the case of the fungal pathogen, spore inoculation meets this purpose; however, spores are unavailable in *R. solani* because its sexual stage rarely occurs on artificial medium. Therefore, we secondary put parafilm sheets between the inoculums and the detached leaves to avoid infection at the contact face. With this procedure, we expected enrichment of synchronous infection events from extended aerial hyphae. Thirdly, we shifted the incubation temperature from 23 to 25 °C which makes the fungus more aggressive.

In this improved inoculation method, extended fungal aerial hyphae from inoculum could be observed at 4 hpi and the whole leaf area was covered with dense hyphae at 16 hours. The timing of symptom appearance was shortened from 72 to 24 hpi compared with the previous method (Figure 2a) (Kouzai *et al.* 2018).

Next, infected leaves with this modified inoculation method were harvested at 2, 4, 6, 10, 16, 24, and 32 hpi and fungal biomass in the infected leaf samples was traced by qRT-PCR using cDNAs synthesized from total RNAs with primer sets for *18S rRNA* gene (Xia *et al.* 2017). Note that aerial hyphae on leaf surfaces were removed using both adhesive surgical tape and wet paper wipers with 70% ethanol. The fungal *18S rRNA* gene was reproducibly detected from 6 hpi but not 4 hpi or earlier and its level massively increased during infection up to 32 hpi (Figure 2b).

Table 1. Primers used in this study to validate the inoculation test

| Gene | Primer sequence | Gene Description |
|-------------|---|---|
| 18S | AATTCCAGCTCCAATAGCGT TACATACCGTGAGGCAGACC | rRNA marker gene for fungal biomass quantification |
| AG1IA_05310 | CAACAAGAAAAGTTCACCGAGTATG CGACTTTCGGTTCGTTTG | cytochrome C oxidase assembly protein CtaG/cox11 domain |
| AG1IA_06618 | GCGGGGTTAGTTGTGGTTG GGCTTCATAGCAGGGGAAAAG | Pectate lyase family 1 |
| AG1IA_06890 | ACCAGGACCACGACAAGGAC TGCTATCCGAGTGCCCAAC | Pectate lyase family 1 |
| AG1IA_07787 | TCCCTTTTCGTTTCAGTGTAGTTAGG TTATTGGGCAGGATCGTTTTG | Glycoside hydrolase family 31 |
| AG1IA_07795 | GGATCAACTGGGCAACTCAAC GCAGCTACTACAACATGCACACC | peptidase inhibitor I9 domain |
| AG1IA_08771 | AGACCAGTACGCCTTCACCAC CCCGATAAGCAACCAGAACC | Glycoside hydrolase family 5 |
| AG1IA_09161 | GCCCATACGCTCTTCCAAAC CACCCAACAGCGACTTCATC | Glycosyltransferase GT family 2 domain |

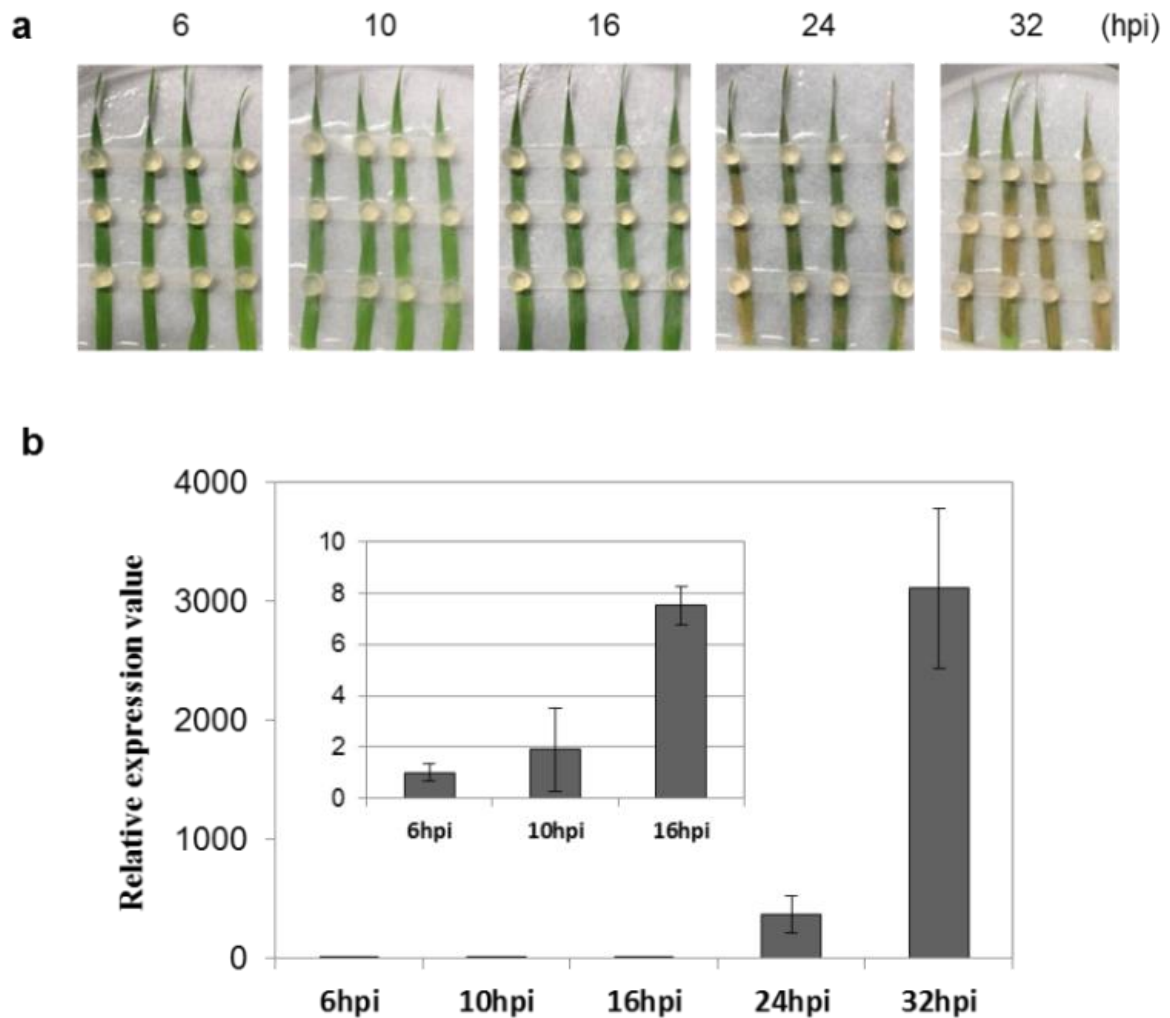


Figure 2. The improved inoculation method of *Rhizoctonia solani* on *Brachypodium distachyon*. **(a)** Progression of infection and symptom appearance in the inoculation method. Leaves detached from 3 weeks old *B. distachyon* were placed in a Petri dish with moist paper and 3 agar plugs prepared from *R. solani*-grown PDA medium were placed on each leaf. The dishes were covered with lids and incubated at 25 °C. Photos were taken at the indicated hours after inoculation (hpi). **(b)** Inoculated leaves were sampled at the indicated timing and hyphae around leaves were removed before the extraction of total RNAs. The relative abundance of fungal biomasses of the infected tissues was measured by qRT-PCR using cDNAs prepared from extracted RNAs with a specific primer for *18S rRNA* marker gene.

Table 2. Summary of RNA-sequencing analysis of *Rhizoctonia solani* during the infection stages on detached leaves of *Brachypodium distachyon* (Accession Bd21)

| Accession | Hours post inoculation (hpi) | Biological replicates | Number of total reads | Mapped to <i>B. distachyon</i> Bd21 genome | | | Number of unmapped reads against Bd21 genome | Discarded reads in unmapped reads against Bd21 genome (single reads) | Mapped to <i>R. solani</i> genome | | | | |
|-----------|------------------------------|-----------------------|-----------------------|--|--------------------------|-----------------------------------|--|--|-----------------------------------|------------------------|--------------------------|---------------------------------|-----------------------------------|
| | | | | Number of mapped reads | Rate of mapped reads (%) | Rate of properly paired reads (%) | | | Number of total reads | Number of mapped reads | Rate of mapped reads (%) | Number of properly paired reads | Rate of properly paired reads (%) |
| Bd21 | 0 | 1 | 52,207,984 | 49,720,087 | 95.23 | 85.57 | 2,487,897 | 1,186,555 | 1,301,342 | 288 | 0.022 | 200 | 0.015 |
| | | 2 | 49,850,060 | 47,238,949 | 94.76 | 86.17 | 2,611,111 | 1,300,123 | 1,310,988 | 334 | 0.025 | 222 | 0.017 |
| | | 3 | 59,621,170 | 56,432,120 | 94.65 | 86.47 | 3,189,050 | 1,428,594 | 1,760,456 | 629 | 0.036 | 466 | 0.026 |
| | 8 | 1 | 51,894,736 | 48,761,392 | 93.96 | 85.98 | 3,133,344 | 1,320,408 | 1,812,936 | 36,066 | 1.989 | 30,258 | 1.669 |
| | | 2 | 64,192,412 | 60,122,908 | 93.66 | 85.26 | 4,069,504 | 1,589,254 | 2,480,250 | 13,589 | 0.548 | 11,340 | 0.457 |
| | | 3 | 60,687,308 | 56,567,307 | 93.21 | 83 | 4,120,001 | 1,533,021 | 2,586,980 | 11,334 | 0.438 | 9,098 | 0.352 |
| | 16 | 1 | 66,301,522 | 62,589,364 | 94.4 | 84.36 | 3,712,158 | 1,621,656 | 2,090,502 | 28,194 | 1.349 | 23,248 | 1.112 |
| | | 2 | 54,712,438 | 51,597,948 | 94.31 | 84.16 | 3,114,490 | 1,422,726 | 1,691,764 | 177,838 | 10.512 | 146,494 | 8.659 |
| | | 3 | 54,583,756 | 51,832,740 | 94.96 | 84.46 | 2,751,016 | 1,250,526 | 1,500,490 | 71,614 | 4.773 | 58,730 | 3.914 |
| | 24 | 1 | 63,467,542 | 59,425,895 | 93.63 | 82.87 | 4,041,647 | 1,465,835 | 2,575,812 | 424,307 | 16.473 | 350,494 | 13.607 |
| | | 2 | 68,187,874 | 63,431,440 | 93.02 | 85.61 | 4,756,434 | 1,537,080 | 3,219,354 | 317,874 | 9.874 | 274,380 | 8.523 |
| | | 3 | 66,037,546 | 61,179,420 | 92.64 | 81.25 | 4,858,126 | 1,411,340 | 3,446,786 | 1,509,515 | 43.795 | 1,260,664 | 36.575 |

Evaluation of the inoculation system with characterized genes

Zheng *et al.* (2013) performed dual RNA-seq analysis using infected rice plants with *R. solani* AG-1 IA. Expression profiles of *R. solani* genes encoding carbohydrate-active enzymes (CAZyme) possibly involved in fungal pathogenicity have been characterized. We selected *AGIIA_08771* (Glycoside hydrolase family 5), *AGIIA_06618* (Pectate lyase family 1), *AGIIA_06890* (Pectate lyase family1), and *AGIIA_07787* (Glycoside hydrolase family 31) and tested their expressions in our infection system. Expression of *AGIIA_08771*, which was reported to express at 18, 24, and 72 hpi, was detected with a peak at 6 hpi in our system. While, the transcriptions of the other genes, whose expression timings are at 24–72 hpi on rice, were observed at a later stage such as 24 and 32 hpi on *B. distachyon* (Figure 3a) and they were almost consistent. The 48–72 hpi on rice experiment appeared to correspond to the 24–32 hpi in our modified inoculation using *Brachypodium* system. Next, we also examined expression profiles of secretory proteins *AGIIA_07795* (peptidase inhibitor I9 domain), *AGIIA_091651* (glycosyltransferase GT family 2 domain), and *AGIIA_05310* (cytochrome C oxidase assembly protein CtaG/cox11 domain) which could induce necrotic lesions when their purified proteins were injected into leaves of rice and maize (Zheng *et al.* 2013). Their transcripts were also detected during the infection in *B. distachyon* (Figure 3b). The expression timings of *AGIIA_07795*, *AGIIA_091651*, and *AGIIA_05310* in rice infection were 18–24 (mainly at 24), 24–32 (mainly at 24), and 24–32 (mainly at 32) hpi, respectively. In our pathosystem, their expression peaks were at 6, 24, and 32 hpi, respectively. Thus, their expression profiles on rice and *Brachypodium* were proportional as well.

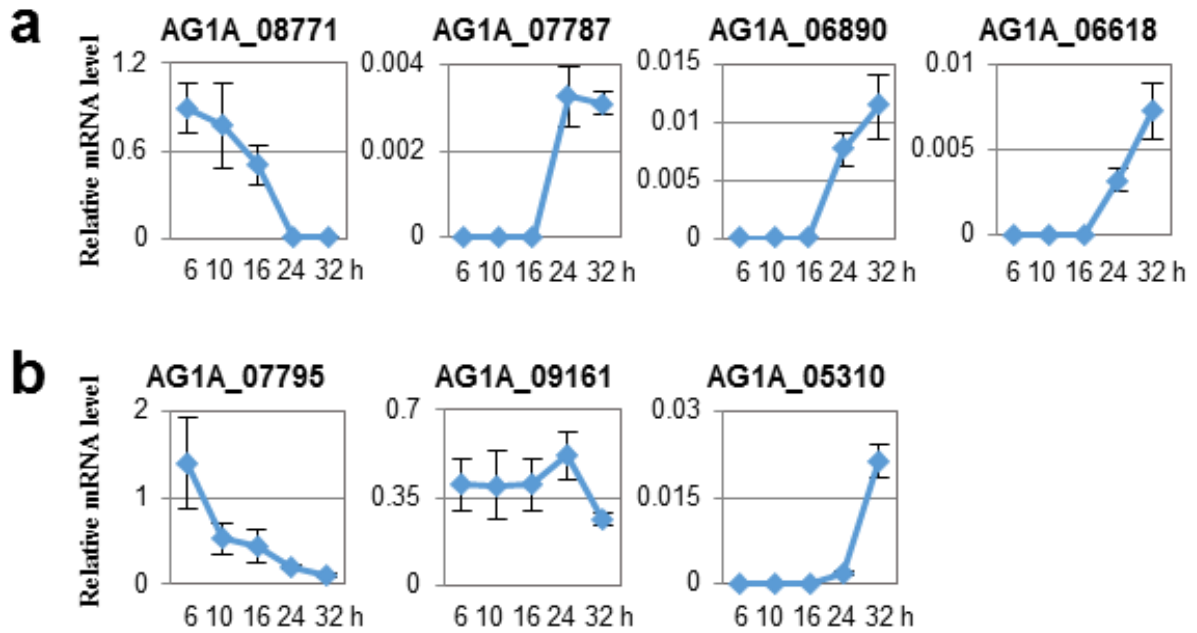


Figure 3. Evaluation of the inoculation method using *Rhizoctonia solani* genes whose expression patterns during inoculation on rice plants have been characterized. (**a** and **b**) Expression patterns of 4 genes (*AG1A_08771*, *AG1A_07787*, *AG1A_06890*, and *AG1A_06618*) encoding carbohydrate-active enzymes (**a**) and 3 secretory effector-like protein genes (*AG1A_07795*, *AG1A_09161*, and *AG1A_05310*) (**b**) of *R. solani* on *Brachypodium distachyon*. Gene expressions were examined using qRT-PCR using cDNA prepared from total RNAs extracted from *R. solani*-inoculated *B. distachyon* leaves at 6, 10, 16, 24, and 32 hpi. Graphs display the relative mRNA level of each gene normalized by *18S rRNA* as an internal control. The data are presented as means with the standard error of 4 biological replicates. Experiments were performed twice with similar results and a representative result is shown.

Discussion

R. solani infection is greatly affected by various environmental factors such as temperature, humidity, and the fungal load in the field (Ogashi 1987). The sensitivity of the fungal organisms' quantification methods is primarily depends on the fungal concentration in the sample tested (Tsui *et al.* 2011). Plant pathogens interact with their host plants in sequential events in which gene expression is tightly regulated (Zeilinger *et al.* 2016). The number of propagules penetrating the plant tissue in the initial infection step is limited. Therefore, the synchronous growth of the pathogen in the artificial infection is vital to detect the early infection events. In this study, transcriptome analysis of infected *B. distachyon* leaves with a single agar inoculum of *R. solani* could not detect significant read counts for the differentially expressed genes during infection at 8 hours post-infection. That is because, in the early infection events, most of the extracted RNA is derived from plants; on the contrary, the fungal-originated RNA is very limited. That makes the detection and identification of the genes involved in the early infection events more difficult (Ghosh *et al.* 2014). Additionally, spores are not available in this fungus, therefore, it is not easy to maintain the normal synchronized growth of this fungus *in vitro* with the simple detached leaf assay.

To overcome the scarcity of pathogen-derived RNA reads in RNA-seq analysis of the infected plants, researchers in the plant pathology disciplines tried to enhance the detection efficiency (Asai *et al.* 2014, Nobori *et al.* 2018). In this study, we modified the infection method developed by Kouzai *et al.* 2017. Simply I increased the number of inocula on a restricted leaf area for infection. Also, qRT-PCR was used as a detection method for transcripts to expect higher sensitivity. For this purpose, controlling the synchronicity of the infection should have a great effect on the results. A plant sample of the broad infected area with a single inoculum should contain varied infection stages from extended aerial hyphae. In our improved inoculation method, extended aerial hypha quickly overlays a small open area of detached leaf blades, therefore, it may enable to concentrate synchronous infection event as much as possible. The controlled high humidity condition with covered Petri dish also must contribute to stable and uniform infection. In this method, the fungal *18S rRNA* gene was reproducibly detected from 6 hpi and its level massively increased during infection up to 32 hpi. Therefore, this method will be useful for early detection. The expression patterns of the selected cell wall degrading enzyme genes were almost consistent on both rice and *B. distachyon*. Effector proteins are known to suppress plant immunity, especially in the early infection events (Glazebrook 2005). The expression patterns of three effector protein genes previously detected

by Zheng *et al.* 2013 using the simple detached inoculation method were also consistent with their expression using the newly developed method. Therefore, this method is useful to precisely detect the genes expressed in the infection events even in the early infection step. Additionally, the uniformity of the selected genes' expression patterns means that *R. solani* uses the same infection strategy to invade both plants.

References

- Anderson, N.A. The Genetics and Pathology of *Rhizoctonia Solani*. Annu. Rev. Phytopathol. 20, 329–347 (1982).
- Applied Biosystems. (1997) Relative quantitation of gene expression: ABI PRISM 7700 Sequence Detection System: User Bulletin #2: Rev B. (*AppliedBiosystems P/N 4303859*).
- Aregbesola, E. *et al.* A detached leaf assay to rapidly screen for resistance of maize to *Bipolaris maydis*, the causal agent of southern corn leaf blight. Eur. J. Plant Pathol. 156, 133–145 (2020).
- Arraiano, L.S., Brading, P.A. & Brown, J.K.M. A detached seedling leaf technique to study resistance to *Mycosphaerella graminicola* (anamorph *Septoria tritici*) in wheat. Plant Pathol. 50, 339–346 (2001).
- Asai, S. *et al.* Expression profiling during Arabidopsis/downy mildew interaction reveals a highly-expressed effector that attenuates responses to salicylic acid. PLoS Pathog. 10, e1004443 (2014).
- Fenille, R.C., Ciampi, M.B., Kuramae, E.E. & Souza, N.L. Identification of *Rhizoctonia solani* associated with soybean in Brazil by rDNA-ITS sequences. Fitopatol. Bras. 28, 413–419 (2003).
- Ghosh, S., Gupta, S.K. & Jha, G. Identification and functional analysis of AG1-IA specific genes of *Rhizoctonia solani*. Curr. Genet. 60, 327–341 (2014).
- Glazebrook, J. Contrasting mechanisms of defense against biotrophic and necrotrophic pathogens. Annu. Rev. Phytopathol. 43, 205–227 (2005).
- Hashiba, T. Estimation method of severity and yield loss by rice sheath blight disease. Bull. Hokuriku Natl. Agric. Exp. Station 26, 115–164 (1984).
- Kim D., Pertea G., Trapnell C., Pimentel H., Kelley R. & Salzberg, S.L. TopHat2: accurate alignment of transcriptomes in the presence of insertions, deletions, and gene fusions. Genome Biol. 14, R36 (2013).
- Kouzai, Y. *et al.* Salicylic acid-dependent immunity contributes to resistance against *Rhizoctonia solani*, a necrotrophic fungal agent of sheath blight, in rice and *Brachypodium distachyon*. New Phytol. 217, 771–783 (2018a).
- Lakshman, D.K., Alkharouf, N., Roberts, D.P., Natarajan, S.S. & Mitra, A. Gene expression profiling of the plant pathogenic basidiomycetous fungus: *Rhizoctonia solani* AG 4 reveals putative virulence factors. Mycologia 104, 1020–1035 (2012).

- Langmead, B. & Salzberg, S.L. Fast gapped-read alignment with Bowtie 2. *Nat. Methods* 9, 357–359 (2012).
- Lee, F. N & Rush, M.C. Rice sheath blight: A major rice disease. *Plant Dis.* 67, 829–832 (1983).
- Mazzola, M., Wong, O.T. & Cook, R.J. Virulence of *Rhizoctonia oryzae* and *R. solani* AG-8 on wheat and detection of *R. oryzae* in plant tissue by PCR. *Phytopathology* 86, 354–360 (1996).
- Nobori, T. *et al.* Transcriptome landscape of a bacterial pathogen under plant immunity. *Proc. Natl. Acad. Sci. U. S. A.* 115, E3055–E3064 (2018).
- Ogoshi, A. Ecology and pathogenicity of anastomosis and intraspecific groups of *Rhizoctonia solani* Kuhn. *Annu. Rev. Phytopathol.* 25, 125–143 (1987).
- Sayler, R.J. & Yang, Y. Detection and quantification of *Rhizoctonia solani* AG-1 IA, the rice sheath blight pathogen, in rice using real-time PCR. *Plant Dis.* 91, 1663–1668 (2007).
- Trapnell, C. *et al.* Differential gene and transcript expression analysis of RNA-seq experiments with TopHat and Cufflinks. *Nat. Protoc.* 7, 562–578 (2012).
- Tsui, C.K.M., Woodhall J., Chen W., Lévesque, C.A., Lau A., Schoen C.D., Baschien C., Najafzadeh M.J. & de Hoog, S.G. Molecular techniques for pathogen identification and fungus detection in the environment. *IMA Fungus* 2, 177–189 (2011).
- Untergasser, A. *et al.* Primer3-new capabilities and interfaces. *Nucleic Acids Res.* 40, e115 (2012).
- Uppala, S. & Zhou, X.-G. Rice sheath blight. *Plant Heal. Instr.* (2018) doi:10.1094/PHI-I-2018-0403-01.
- Xia, Y. *et al.* Transcriptome analysis reveals the host selection fitness mechanisms of the *Rhizoctonia solani* AG1IA pathogen. *Sci. Rep.* 7, 10120 (2017).
- Yamamoto, N. *et al.* Integrative transcriptome analysis discloses the molecular basis of a heterogeneous fungal phytopathogen complex, *Rhizoctonia solani* AG-1 subgroups. *Sci. Rep.* 9, 19626 (2019).
- Zeilinger, S. *et al.* Friends or foes? Emerging insights from fungal interactions with plants. *FEMS Microbiol. Rev.* 40, 182–207 (2016).
- Zheng, A. *et al.* The evolution and pathogenic mechanisms of the rice sheath blight pathogen. *Nat. Commun.* 4, 1424 (2013).

Chapter 3

Identification of effector protein genes from *Rhizoctonia solani* using the publicly available genome sequence and bioinformatics tools

Abstract

Rhizoctonia solani is a widely distributed fungus infecting several host plants. This fungus is known to use a vast array of genes that are involved in its pathogenicity. In general, effectors are secreted protein and essential weapons deployed by plant pathogens to invade and manipulate host defenses. Identifying such protein is critical for understanding the infection mechanisms of plant pathogens and such knowledge could be ultimately applied to reduce crop losses. The availability of the next generation sequences nowadays has facilitated the whole genome sequencing for many plant pathogens. Several bioinformatics tools are freely available for effector prediction. As a direct impact of these genomic data and bioinformatics tools, identifying effector protein genes from many plant pathogens becomes easier. In this study, Effector protein-encoding candidate genes were predicted from the genome of *R. solani* to understand its role in the infection process. Several bioinformatics tools (EffectorP, SignalP, TargetP, big-PI, and PredGPI) were employed as pipelines for effector protein gene identification. The potential effector protein genes of *R. solani* were extracted from its publicly available genome sequence using these tools. The tools used in this study can discriminate potential effector proteins with a signal peptide for secretion from the fungal secretomes. Out of 10,541 proteins, 88 genes were identified as a potential effector protein gene, and they were named *R. solani* secretory effector-like protein genes (*RsSEPGs*).

Introduction

R. solani AG-1 IA causing sheath blight, a severe disease, leads to significant losses in rice fields. To prevent the plant pathogen's agricultural damages, a better understanding of the pathogenicity and virulence factors is essential to develop countermeasures such as disease resistance cultivars, virulence-suppressing chemicals, or defense-activating compounds (Sonah *et al.* 2016). Plant pathogens have developed sophisticated mechanisms to overcome plant defense responses. Initially, plants use transmembrane pattern recognition receptors to sense the microbe or pathogen-associated molecular patterns (MAMPs or PAMPs), thereby activating defense response so-called Pattern-triggered immunity (PTI) (Jones and Dangl 2006). In turn, plant pathogens produce a wide range of bioactive molecules such as enzymes, proteins, peptides, secondary metabolites, effectors, and toxins, which are crucial chemical tools for the successful invasion of host plants (Agrios 2005, Vincent *et al.* 2020). Pathogen's effector proteins are known to inhibit host components involved in PTI. To counteract this pathogen's action, plants deploy the resistance (*R*) genes that encode nucleotide-binding and leucine-rich repeats (NB-LRR) proteins as the second wave of an immune response. NB-LRR proteins, in turn, recognize diverse effectors from different pathogens directly or indirectly and, therefore, activate defense responses named effector-triggered immunity (ETI) (Jones and Dangl 2006, Morgan and Kamoun 2007, Li *et al.* 2019). ETI is associated with the massive production of many secondary metabolites or proteins with antimicrobial activities, which are crucial for resistance. These compounds include reactive oxygen, chitinases, phytoalexins, and glucanases (Giraldo and Valent 2013).

Effectors evolve quickly; therefore, mutations or complete loss of a particular effector has been observed (S´anchez-Vallet *et al.* 2018). Consequently, plants lose their ability to recognize effectors, and it was recognized as the brake of disease resistant cultivars in the field (Jones and Dangl 2006, Giraldo and Valent 2013). Hence, effector protein genes are crucial topics to be considered for the understanding of pathogen virulence and plant immunity.

The effector protein definition is still controversial in the field of plant pathology (Sourico 2013, Sonah *et al.* 2016). In general, effectors are plant-pathogen secreted molecules that alter host cell structure and function to cause/facilitate infection, trigger defense responses, or avoid recognition by the host plant (Kamoun 2006, Sourico 2013). Therefore, the term effector is used in a broad sense to describe several molecules, including carbohydrates, secondary metabolites, which are involved in the infection process. The identification of effector proteins depends on several characteristics. Several features are being used to identify

effector proteins such as small size, signal peptide for secretion, no trans-membrane domains, cysteine-rich, and similarity with other protein domains (Sperschneider *et al.* 2016). Effectors contain a signal peptide of variable size up to 60 amino acids followed by a cleavage site and C-terminus. These criteria have been employed to identify effector protein genes using computational algorithms. Therefore, BLAST search alone cannot function properly for effector prediction (Sonah *et al.* 2016, Sperschneider *et al.* 2016). Petersen *et al.* 2011 reported the importance of using SignalP to predict the secretory proteins with the signal peptide. Secreted effector proteins should not have transmembrane domains or glycosylphosphatidylinositol (GPI) anchored motifs, sophisticated tools such as PredGPI can be used to exclude such transmembrane- or membrane-anchored proteins from the effector candidates (Pierleoni *et al.* 2008, Sonah *et al.* 2016). For this purpose, THMM which uses a hidden Markov-based method is also applicable (Krogh *et al.* 2001). EffectorP is an online tool that was developed based on machine learning by Sperschneider *et al.* 2016 to predict the effector proteins from the fungal secretomes with sensitivity and specificity of over 80%. Using these pipelines can increase the accuracy of the prediction of effector proteins.

Many secretory proteins have been identified from different plant pathogenic fungi so far (Zheng *et al.* 2013, Anderson *et al.* 2017, Li *et al.* 2019). In this study, a set of bioinformatics tools were used to predict the effector candidate genes of *R. solani* which is designated as *R. solani* secretory effector-like protein genes (*RsSEPGs*). The annotated amino acid sequences of the *R. solani* publicly available genome sequence was used. Then, the *RsSEPGs* encoding potential effectors were predicted using the above-mentioned bioinformatics tools. Out of 10,541 proteins, 88 genes were selected as *RsSEPGs*. This investigation opens new avenues for the functional analysis of *R. solani* effector proteins.

Materials and methods

Identification of *R*sSEPGs

Annotated protein sequences of *R. solani* AG-1 IA genome obtained from the Ensembl Fungi database (GCA_000334115) were used for searching sequence motifs (Zheng *et al.* 2013). The prediction pipeline in Figure 4 was used for effector prediction. The peptide for eukaryotic secretion signals was predicted using SignalP-4.1 and TargetP-1.1 (Petersen *et al.* 2011, Emanuelsson *et al.* 2000). For transmembrane domain search, TMHMM2.0 and SignalP-4.1 were used (Krogh *et al.* 2001). The GPI-anchoring motif was detected using PredGPI (Pierleoni *et al.* 2008). To obtain predictions as fungal effectors, EffectorP 1.0 was employed (Sperschneider *et al.* 2016).

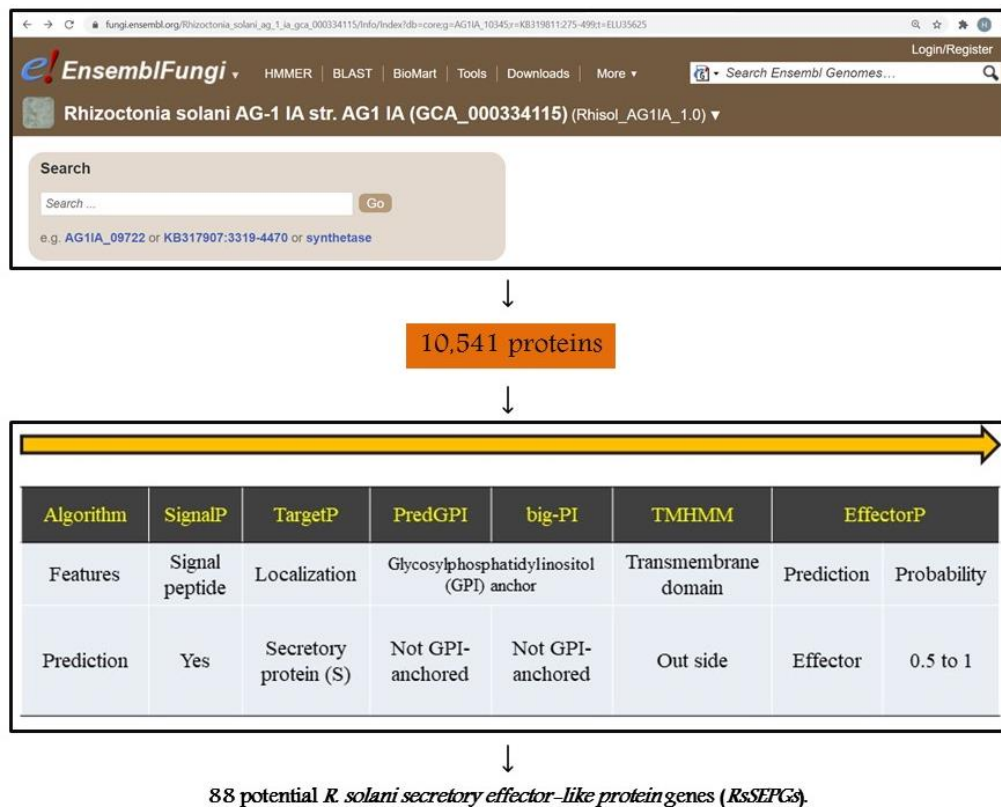


Figure 4. The pipeline used for effector prediction from the annotated protein sequences of *R. solani*. The proteins of 10,541 genes of the assembled genome of *R. solani* was retrieved from EnsemblFungi database (Upper panel). Bioinformatics tools (SignalP, TargetP, PredGPI, big-PI, TMHMM, and EffectorP) were used to search for effector characteristics (Lower panel) (Signal peptide, outside localization, no GPI-anchored, no transmembrane domain, expressed *in planta*, small size, and high cysteine content). Out of the total, 88 potential *R*sSEPGs were selected based on these features.

Results

Surveillance of *secretory effector-like protein genes (RsSEPGs)* in *R. solani*

Using publicly available deduced protein sequences determined by gene annotation of *R. solani* AG-1 IA (Zheng *et al.* 2013), we surveyed effector candidate genes. To select potential secretory proteins, SignalP 4.1 and TargetP 1.1 programs were used, and proteins possessing eukaryotic signal peptides for secretion were extracted (Petersen *et al.* 2011, Emanuelsson *et al.* 2007). To exclude membrane-localized proteins, we used TMHMM and SignalP 4.1 (Krogh *et al.* 2001). Then, possible membrane-associated proteins with GPI-anchoring motif were detected using the PredGPI algorithm, and they were removed (Pierleoni *et al.* 2008). Finally, EffectorP 1.0 program was applied to select fungal effector candidates (Figure 5) such as small size and high cysteine content proteins (Sperschneider *et al.* 2016). Of the total 10,541 proteins, 88 proteins satisfied the above-mentioned all criteria, and they were designated as *R. solani* *secretory effector-like protein genes (RsSEPGs)* (Table 3).

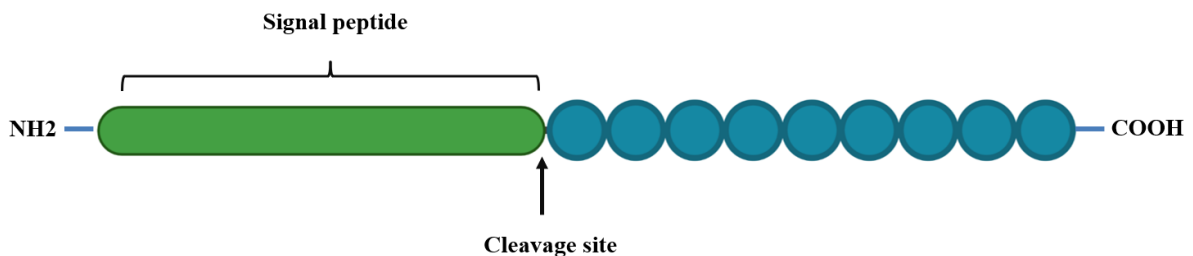


Figure 5. The protein organization of the potential *RsSEPGs* with signal peptide, cleavage site and the functional C-terminus region.

Table 3. The potential predicted *secretory effector-like protein genes (RsSEPGs)* in *R. solani* AG-1 IA

| Gene ID | Annotation | Gene ID | Annotation |
|-------------|---|-------------|---|
| AG1IA_00153 | hypothetical protein | AG1IA_06710 | hypothetical protein |
| AG1IA_00157 | polysaccharide deacetylase domain-containing protein | AG1IA_06739 | hypothetical protein |
| AG1IA_00172 | hypothetical protein | AG1IA_06741 | hypothetical protein |
| AG1IA_00273 | hypothetical protein | AG1IA_07047 | hypothetical protein |
| AG1IA_00431 | GILT domain-containing protein | AG1IA_07075 | CFEM domain-containing protein |
| AG1IA_00478 | hypothetical protein | AG1IA_07122 | hypothetical protein |
| AG1IA_00529 | hypothetical protein | AG1IA_07262 | hypothetical protein |
| AG1IA_00669 | glycosyl hydrolase family 61 domain-containing protein | AG1IA_07267 | hypothetical protein |
| AG1IA_00684 | hypothetical protein | AG1IA_07490 | Yippee domain-containing protein |
| AG1IA_00763 | hypothetical protein | AG1IA_07958 | igA peptidase m64 domain-containing protein |
| AG1IA_00879 | hypothetical protein | AG1IA_07966 | hypothetical protein |
| AG1IA_00951 | deuterolysin metalloprotease (M35) family domain-containing protein | AG1IA_08025 | hypothetical protein |
| AG1IA_01042 | hypothetical protein | AG1IA_08061 | hypothetical protein |
| AG1IA_01512 | hypothetical protein | AG1IA_08487 | Ribonuclease domain-containing protein |
| AG1IA_01599 | lipoic acid synthase | AG1IA_08488 | Ribonuclease domain-containing protein |
| AG1IA_01603 | hypothetical protein | AG1IA_08615 | hypothetical protein |
| AG1IA_01604 | hypothetical protein | AG1IA_08650 | hypothetical protein |
| AG1IA_01605 | hypothetical protein | AG1IA_08777 | plastocyanin-like domain-containing protein |
| AG1IA_01933 | hypothetical protein | AG1IA_08781 | hypothetical protein |
| AG1IA_02138 | hypothetical protein | AG1IA_08891 | hypothetical protein |
| AG1IA_02490 | hypothetical protein | AG1IA_08892 | hypothetical protein |
| AG1IA_02879 | hypothetical protein | AG1IA_08957 | hypothetical protein |
| AG1IA_02940 | hypothetical protein | AG1IA_09055 | thaumatin-like protein |
| AG1IA_03047 | hypothetical protein | AG1IA_09060 | thaumatin-like protein |
| AG1IA_03254 | hypothetical protein | AG1IA_09196 | hypothetical protein |
| AG1IA_04006 | hypothetical protein | AG1IA_09202 | hypothetical protein |
| AG1IA_04108 | hypothetical protein | AG1IA_09203 | hypothetical protein |
| AG1IA_04191 | hypothetical protein | AG1IA_09207 | hypothetical protein |
| AG1IA_04237 | hypothetical protein | AG1IA_09229 | hypothetical protein |
| AG1IA_04268 | hypothetical protein | AG1IA_09275 | hypothetical protein |
| AG1IA_04298 | emp24/gp25L/p24 family/GOLD domain-containing protein | AG1IA_09529 | hypothetical protein |
| AG1IA_04737 | hypothetical protein | AG1IA_09643 | hypothetical protein |
| AG1IA_04814 | hypothetical protein | AG1IA_09728 | hypothetical protein |
| AG1IA_04819 | fungal cellulose binding domain-containing protein | AG1IA_09836 | hypothetical protein |
| AG1IA_04889 | hypothetical protein | AG1IA_09837 | hypothetical protein |
| AG1IA_05179 | hypothetical protein | AG1IA_09956 | hypothetical protein |
| AG1IA_05291 | hypothetical protein | AG1IA_10146 | hypothetical protein |
| AG1IA_05500 | hypothetical protein | AG1IA_10180 | hypothetical protein |
| AG1IA_05601 | hypothetical protein | AG1IA_10284 | hypothetical protein |
| AG1IA_05783 | hypothetical protein | AG1IA_10296 | hypothetical protein |
| AG1IA_05938 | hypothetical protein | AG1IA_10375 | valine-tRNA ligase |
| AG1IA_06169 | hypothetical protein | AG1IA_10403 | hypothetical protein |
| AG1IA_06325 | FKBP-type peptidyl-prolyl cis-trans isomerase domain-containing protein | AG1IA_10405 | hypothetical protein |
| AG1IA_06613 | hypothetical protein | AG1IA_10478 | hypothetical protein |

Discussion

Plant pathogens have developed sophisticated mechanisms to overcome plant defense responses; secreted effectors are a part of an essential strategy used by plant pathogens to suppress plant immunity (Jones and Dangl 2006). Therefore, their identification and annotation are of great importance to understand the pathogenicity mechanism. In the annotated genome of *R. solani*, various genes encoding potential secretory proteins with pathogenicity such as cell wall lytic enzymes have been reported (Zheng *et al.* 2013). The secretory proteins should contain effector candidates and they are mostly expected to possess unique features such as small size, signal peptide for secretion, no trans-membrane domains, cysteine-rich, and no similarity with other protein domains. (Sonah *et al.* 2016, Sperschneider *et al.* 2016). Several tools have been used for effector prediction, despite their limitations, but using a combination of these tools increase the accuracy of effector prediction (Sonah *et al.* 2016). In this study, 88 effectors were identified using a set of bioinformatics tools. EffectorP, PredGPI, THMM, and SignalP were used to discriminate against the effector candidate proteins from *R. solani* genome. The predicted effector candidate protein genes are relatively small in size and almost have no homologous proteins detected in other organisms (Kamoun 2006, Sonah *et al.* 2016). Several proteins with a predicted function have been identified from different plant pathogenic fungi using these tools (Zheng *et al.* 2013, Anderson *et al.* 2017, Li *et al.* 2019). Some of the predicted effectors (AG1IA_08487 and AG1IA_08488) have similarities with known proteins such as ribonuclease, cellulose-binding domain (AG1IA_04819), thaumatin-like protein (AG1IA_09055 and AG1IA_09060), and CFEM domain-containing protein (AG1IA_07075) (Anderson *et al.* 2016, Pennington *et al.* 2019), function characterization of such proteins could decipher their role in pathogenicity. Zheng *et al.* 2013 reported 145 secreted proteins. At least 3 of them were demonstrated to induce necrosis after their purified protein was infiltrated into rice, maize, and soybean leaves. They were considered as effectors working at a later time point during infection. Because not all the predicted secretory fungal proteins function as effector, prediction of effector candidate and its functional study would be important to characterize fungal virulence-related genes efficiently. The effector candidate genes identified in our investigation opens new avenues for a better understanding of *the R. solani* infection mechanism.

References

- Agrios, G. Plant pathology: Fifth edition. Plant Pathology: Fifth Edition (2004).
- Anderson, J.P. *et al.* Comparative secretome analysis of *Rhizoctonia solani* isolates with different host ranges reveals unique secretomes and cell death inducing effectors. *Sci. Rep.* 7, 10140 (2017).
- Emanuelsson, O., Nielsen, H., Brunak, S. & von Heijne, G. Predicting subcellular localization of proteins based on their N-terminal amino acid sequence. *J. Mol. Biol.* 300, 1005–1016 (2000).
- Giraldo, M.C. & Valent, B. Filamentous plant pathogen effectors in action. *Nat. Rev. Microbiol.* 11, 800–814 (2013).
- Jones, J.D.G. & Dangl J.L. The plant immune system. *Nature* 444, 323–329 (2006).
- Kamoun, S.A. Catalogue of the effector secretome of plant pathogenic oomycetes. *Annu. Rev. Phytopathol.* 44, 41–60 (2006).
- Krogh, A., Larsson, B., Von Heijne, G. & Sonnhammer, E.L.L. Predicting transmembrane protein topology with a hidden Markov model: Application to complete genomes. *J. Mol. Biol.* 305, 567–580 (2001).
- Li, S. *et al.* The effector AGLIP1 in *Rhizoctonia solani* AG1 IA triggers cell death in plants and promotes disease development through inhibiting PAMP-triggered immunity in *Arabidopsis thaliana*. *Front. Plant Sci.* 10, 2228 (2019).
- Morgan, W. & Kamoun, S. RXLR effectors of plant pathogenic oomycetes. *Curr. Opin. Microbiol.* 10, 332–338 (2007).
- Nemri, A. *et al.* The genome sequence and effector complement of the flax rust pathogen *Melampsora lini*. *Front. Plant Sci.* 5, 98 (2014).
- Pennington, H.G. *et al.* The fungal ribonuclease-like effector protein CSEP0064/BEC1054 represses plant immunity and interferes with degradation of host ribosomal RNA. *PLoS Pathog.* 15, e1007620 (2019).
- Petersen, T.N., Brunak, S., Von Heijne, G. & Nielsen, H. SignalP 4.0: Discriminating signal peptides from transmembrane regions. *Nat. Methods* 8, 785–786 (2011).
- Pierleoni, A., Martelli, P. & Casadio, R. PredGPI: A GPI-anchor predictor. *BMC Bioinformatics* 9, 392 (2008).
- Sánchez-Vallet, A. *et al.* The genome biology of effector gene evolution in filamentous plant pathogens. *Annu. Rev. Phytopathol.* 56, 21–40 (2018)
- Sonah, H., Deshmukh, R.K. & Bélanger, R.R. Computational prediction of effector proteins in fungi: Opportunities and challenges. *Front. Plant Sci.* 7, 126 (2016).

- Sperschneider, J. *et al.* Methods EffectorP: Predicting fungal effector proteins from secretomes using machine learning. *New Phytol.* 210, 743–761 (2016).
- SuRiCO, G. The concepts of plant pathogenicity, virulence/avirulence and effector proteins by a teacher of plant pathology. *Phytopathol. Mediterr.* 52, 399–417 (2013).
- Vincent, D., Rafiqi, M. & Job, D. The Multiple facets of plant–fungal interactions revealed through plant and fungal secretomics. *Front. Plant Sci.* 10, 1626 (2020).
- Zheng, A. *et al.* The evolution and pathogenic mechanisms of the rice sheath blight pathogen. *Nat. Commun.* 4, 1424 (2013).

Chapter 4

Calibration of the gene model of *RsSEPGs* with RNA-seq data

Abstract

Plant pathogens are a significant threat in crop cultivation worldwide. By secreting various chemical bioactive molecules and proteins, they can perturb plant immunity and eventually cause diseases. One of the crucial secreted molecules is effector proteins, however, deep understanding about their functions is still lagging. The genome biology of the phytopathogenic fungi provides insight into effectors in evolutionary literature. Genes encoding these effectors are rapidly evolving within the genome of the pathogens. Effectors can be gained by gene duplication or by getting a secretion signal. Using such mechanisms, plant pathogens could break the plant resistance or could infect new hosts. In the case of *R. solani*, its virulence was believed to largely rely on necrosis-inducing factors because it is a necrotrophic pathogen. Therefore, many studies focused on secretory proteins but not effectors. However, recent studies using *B. distachyon* demonstrated that *R. solani* may have a short window of the biotrophic process during infection. This means that *R. solani* must employ effector proteins to suppress host immunity for entry. Effector proteins of *R. solani* were successfully predicted by using several tools in chapter 3. Each gene model (Exon-Intron structures) was determined by a computational approach but I found that to be inaccurate. Therefore, the gene models of the selected 88 *RsSEPGs* were calibrated by the RNA-sequencing data obtained from *R. solani* growing on the PAD medium. After the remodeling of the gene structures of *RsSEPGs* and validating transcripts in the reverse strands of each gene, 61 genes were finally chosen for further studies.

Introduction

R. solani is a considered species complex that causes necrotic diseases in a wide range of crops including cereals, the widely used food commodities (Ogashi 1987, Lee and Rush 1983, Zheng *et al.* 2013). To understand the virulence, lifestyle, and evolutionary aspects of the pathogen, whole-genome sequencing data is necessary. Recent progress in the development of next-generation sequencing technology enables us to obtain whole-genome data of any organism. Once whole-genome sequencing data is obtained, genes contained in the genome can be predicted by using informatics tools (Zhao *et al.* 2013, Steele *et al.* 2014). However, de novo intron-exon prediction seems to be a challenging process due to genetic variations (Shen *et al.* 2011). Gene annotation, in most cases, was predicted merely using algorithmic programs. Consequently, there is a high possibility of false-positive gene annotation (Zhao *et al.* 2013).

In the case of *R. solani*, genome assemblies of several isolates from different anastomosis groups have been released (Zheng *et al.* 2013, Wibberg *et al.* 2016, Wibberg *et al.* 2017). The predicted gene models are also available. In addition, comprehensive transcriptome data obtained by using RNA-sequencing also help understanding biological events. Using this technique, transcriptome analysis during infection has been performed in *R. solani* (Zheng *et al.* 2013, Anderson *et al.* 2017, Yamamoto *et al.* 2019). The genomics approach was used to characterize the genetic diversity among *R. solani* isolates belongs to the same anastomosis (AG-1 IA) which is derived from the heterozygosity and multinucleate nature (Yamamoto *et al.* 2019).

By using the publicly available genome sequencing data and its gene annotations, *RsSEPGs* were selected using several bioinformatics tools as shown in chapter 3. However, I realized that the gene models of the identified *RsSEPGs* were not accurate. Therefore, their gene models were further calibrated using RNA-sequencing data obtained from *R. solani* hyphae growing on the PAD medium. By this process, annotations of 57 genes were corrected and 20 of them lost their signal peptide sequence in the revised gene models. This analysis also provides information about transcripts in the reverse strand of each *RsSEPGs* and 7 genes were revealed to have transcripts on their reverse strands. After removing these genes from the initial list, 61 genes were chosen for further studies.

Materials and methods

RNA-seq analysis from *R. solani* and gene calibration

Total RNA was extracted from the mycelia of *R. solani* grown on PDA medium for 72h using the Nucleospin RNA plant kit (TakaraBio) with three biological replicates. The extracted RNA's quality and quantity were checked using a NanoDrop OneC (Thermo Fisher Scientific) and a 2100 Bioanalyzer (Agilent). According to the manufacturer's instructions, libraries for RNA - seq were prepared using a Truseq RNA library preparation kit (Illumina). The prepared libraries were sequenced with Hiseq4000 (Illumina). The obtained reads were mapped to the *R. solani* genome (GCA_000334115) retrieved from Ensemble Fungi using TopHat v2.1.1 with Bowtie v2.2.6 as its mapping tool (Langmead and Salzberg 2012, Kim *et al.* 2013). Single reads were discarded, and the number of mapped reads of each *R. solani* gene was counted and normalized by fragments per kilobase of transcript per million mapped reads (FPKM) using Cufflinks (Trapnell *et al.* 2012). Using the integrative genome viewer (IGV) (Figure 5) (Thorvaldsdottir *et al.* 2012), the RNA sequence reads for the 88 predicted *RsSEPG* were compared with their cognate reference gene from the genome (GCA_000334115) of *R. solani* reported by Zheng *et al.* 2013 to validate their exon-intron structure.

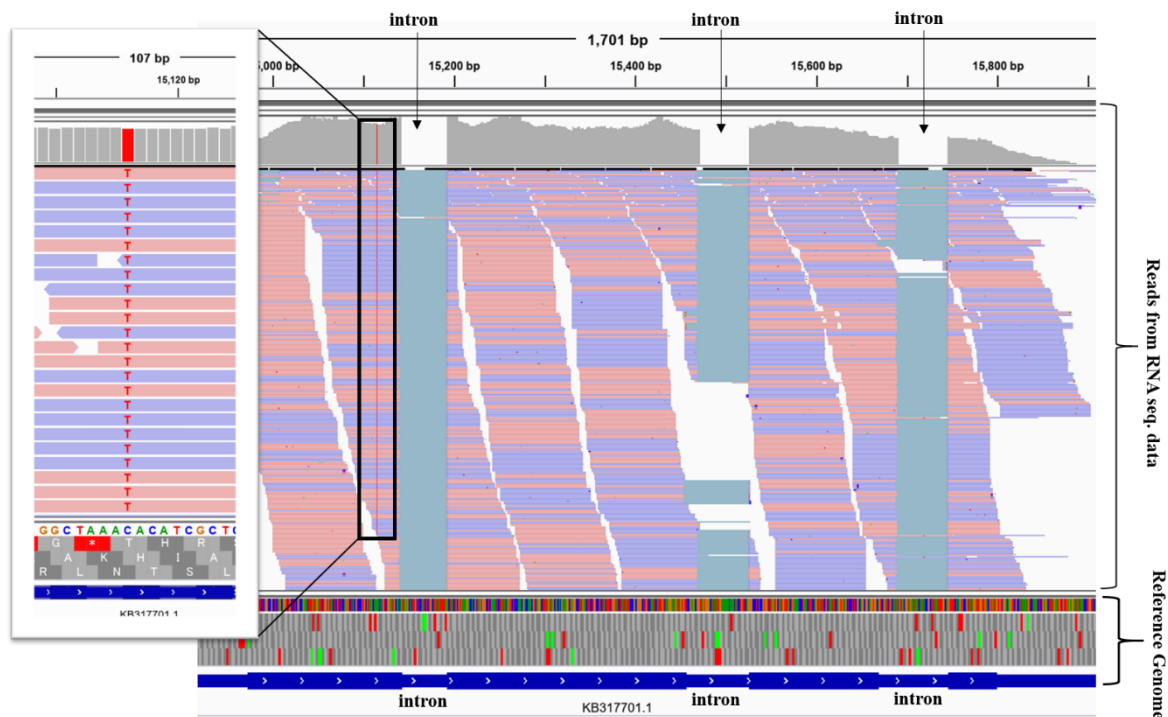


Figure 6: An example of reads alignment view showing different data depending on the zoom level displayed by IGV. The summary of the obtained reads indicated as a coverage plot at 1.7 kb resolution displays the gene structure (Exon-Intron) (Right panel). Reads alignment view at 100 bp resolution reveals the individual base mismatches (Left panel).

Results

Correction of *RsSEPGs* annotations by calibration of gene model with RNA-sequencing data

The annotated gene model of the 88 selected *RsSEPG* was verified by RNA-sequencing data obtained from RNA extracted from *R. solani* hyphae grown on PDA medium (Table 4). Out of the total, the annotated gene models of 11 genes were found to be consistent with the RNA-seq data. Fifty-seven genes were corrected based on RNA-sequencing data. Thirteen genes have no reads detected in RNA-seq data. The remaining 7 genes have abundant transcripts in their reverse strand. Therefore, these 7 genes were removed from the list because appropriate measurements of target gene expression are thought to be prevented in further analysis. In addition, in the above-mentioned 57 genes with calibrated annotation, 20 genes lost their secretion signal peptide in their revised gene model; therefore, they were also removed from the list. In summary, 27 genes were removed from the 88 selected *RsSEPG* and the remaining 61 genes were finally chosen as *RsSEPGs* (Table 5).

Table 4. Summary of RNA-sequencing analysis of *Rhizoctonia solani* growth stage on PDA after 72 hpi.

| Growth | Hours post inoculation (hpi) | Biological replicates | Mapped to <i>R. solani</i> genome | | | | |
|--------|------------------------------|-----------------------|-----------------------------------|------------------------|--------------------------|---------------------------------|-----------------------------------|
| | | | Number of total reads | Number of mapped reads | Rate of mapped reads (%) | Number of properly paired reads | Rate of properly paired reads (%) |
| On PDA | 72 | 1 | 75,820,544 | 62,663,857 | 82.65 | 52,149,370 | 68.78 |
| | | 2 | 71,975,102 | 59,730,523 | 82.99 | 48,662,366 | 67.61 |
| | | 3 | 74,022,804 | 60,630,695 | 81.91 | 50,261,484 | 67.90 |

Table 5. Validation of the gene structures of predicted *Rhizoctonia solani* AG-1 IA secretory effector protein genes (*RsSEPGs*)

| GeneID | Correction of gene model | Loss of signal peptide after annotation calibration | Length (aa) | GeneID | Correction of gene model | Loss of signal peptide after annotation calibration | Length (aa) |
|--------------------------------|--------------------------|---|-------------|--------------------------|--------------------------|---|-------------|
| AG1IA_00157 | yes | no | 168 | AG1IA_06739 | yes | no | 221 |
| AG1IA_00172 ^a | n.a. | n.a. | - | AG1IA_06741 | yes | yes | 59 |
| AG1IA_00273 | yes | no | 146 | AG1IA_07047 | yes | no | 154 |
| AG1IA_00431 | no | no | 232 | AG1IA_07075 | yes | no | 117 |
| AG1IA_00478 | yes | no | 90 | AG1IA_07122 | n.a. | n.a. | 133 |
| AG1IA_00529 | yes | yes | 160 | AG1IA_07262 | n.a. | n.a. | 257 |
| AG1IA_00669 ^c | yes | no | 294> | AG1IA_07267 ^c | yes | no | 159 |
| AG1IA_00684 | yes | no | 67 | AG1IA_07490 | yes | yes | 129 |
| AG1IA_00763 | n.a. | n.a. | 68 | AG1IA_07958 ^c | yes | no | 306 |
| AG1IA_00879 | n.a. | n.a. | 156 | AG1IA_07966 | yes | no | 142 |
| AG1IA_00951 | yes | no | 134 | AG1IA_08025 | no | no | 238 |
| AG1IA_01042 | yes | no | 170 | AG1IA_08061 | n.a. | n.a. | 184 |
| AG1IA_01512 | yes | no | 78 | AG1IA_08487 ^c | yes | no | 144 |
| AG1IA_01599 | yes | yes | 391 | AG1IA_08488 | yes | no | 149 |
| AG1IA_01603 | yes | no | 85 | AG1IA_08577 | n.a. | n.a. | 49 |
| AG1IA_01604 | yes | no | 211 | AG1IA_08615 | yes | no | 225 |
| AG1IA_01605 | no | no | 56 | AG1IA_08650 | yes | no | 213> |
| AG1IA_01933 | n.a. | n.a. | 88 | AG1IA_08777 | yes | no | 160 |
| AG1IA_02138 | yes | yes | 290> | AG1IA_08781 ^a | n.a. | n.a. | - |
| AG1IA_02490 ^a | n.a. | n.a. | - | AG1IA_08891 | yes | yes | 147 |
| AG1IA_02878/79/80 ^b | yes | yes | 759 | AG1IA_08892 | yes | yes | 169 |
| AG1IA_02940 | yes | no | 209 | AG1IA_08957 | yes | yes | 32 |
| AG1IA_03047 | n.a. | n.a. | 68 | AG1IA_09055 | yes | no | 265 |
| AG1IA_03254 | no | no | 111 | AG1IA_09060 | yes | no | 253 |
| AG1IA_04006 | no | no | 54 | AG1IA_09137 ^a | n.a. | n.a. | - |
| AG1IA_04108 | yes | yes | 52 | AG1IA_09202 | yes | no | 184 |
| AG1IA_04191 | yes | yes | 98 | AG1IA_09203 | yes | no | 181 |
| AG1IA_04237 | yes | no | 138 | AG1IA_09207 | yes | no | 182 |
| AG1IA_04267/8 ^b | yes | yes | 478 | AG1IA_09229 | yes | no | 99 |
| AG1IA_04298 | yes | no | 218 | AG1IA_09275 | yes | yes | 158 |
| AG1IA_04737 | n.a. | n.a. | 140 | AG1IA_09643 | n.a. | n.a. | 66 |
| AG1IA_04814 | n.a. | n.a. | 145 | AG1IA_09728 | yes | no | 67 |
| AG1IA_04819 | no | no | 151 | AG1IA_09836 | yes | yes | 147 |
| AG1IA_04889 ^a | n.a. | n.a. | - | AG1IA_09837 | n.a. | n.a. | 131 |
| AG1IA_05179 | yes | yes | 60 | AG1IA_09956 | no | no | 84 |
| AG1IA_05291 | no | no | 230 | AG1IA_10146 | yes | no | 82 |
| AG1IA_05500 | yes | no | 227> | AG1IA_10180 | yes | yes | 146 |
| AG1IA_05601 ^a | n.a. | n.a. | - | AG1IA_10284 | yes | no | 80> |
| AG1IA_05783 | no | no | 90 | AG1IA_10296 ^a | n.a. | n.a. | - |
| AG1IA_05938 | yes | no | 189 | AG1IA_10375 | yes | yes | 168> |
| AG1IA_06169 | n.a. | n.a. | 184 | AG1IA_10403 | yes | yes | 152> |
| AG1IA_06325 | no | no | 142 | AG1IA_10405 | yes | yes | 65> |
| AG1IA_06613 ^c | yes | no | 218 | AG1IA_10478 | no | no | 93 |

^a Transcripts were detected in reverse strand of these genes in RNA-seq results.

^b A series of transcript was detected across multiple annotated genes.

^c Prediction as an effector protein with EffectorP 1.0 was lost in the calibrated cDNA sequences of these 6 genes.

n.a., not applicable

Discussion

In this study, the gene models of the predicted 88 *RsSEPGs* were calibrated using RNA-seq data. In this study, 13 genes were not detected in the RNA-seq data and 7 genes could not be validated due to strong transcripts on their reverse strand. In the remaining 68 genes, only 11 genes (16.4%) were shown to have corrected gene models. In other words, the gene models of the 57 genes (83.8%) were fixed. This inaccuracy rate was so surprising result. Although we did not measure accuracy rate for the other type of *R. solani* genes, it is possible that the current computational annotation method for gene model would be fully optimized for relatively short length cDNA. Otherwise, it is not suitable only for effector genes. Further comparison of prediction accuracy among gene types can clarify this point.

Our results suggest that we could not fully identify effector candidate gene in *R. solani*. The candidate genes which were not annotated and the misannotated genes which actually possess secretion signal peptides must exist. Therefore, de novo-assembly of cDNA based on RNA-seq data is promising in the identification of potential new *RsSEPGs* (Yamamoto *et al.* 2019).

References

- Anderson, J.P. *et al.* Comparative secretome analysis of *Rhizoctonia solani* isolates with different host ranges reveals unique secretomes and cell death inducing effectors. *Sci. Rep.* 7, 10410 (2017).
- Chisholm, S.T., Coaker, G., Day, B. & Staskawicz, B.J. Host-microbe interactions: Shaping the evolution of the plant immune response. *Cell* 124, 803–814 (2006).
- Kim D., Pertea G., Trapnell C., Pimentel H., Kelley R. and Salzberg, S.L. TopHat2: accurate alignment of transcriptomes in the presence of insertions, deletions and gene fusions. *Genome Biol.* 14, R36 (2013).
- Lee, F.N & Rush, M.C. Rice Sheath Blight: A major rice disease. *Plant Dis.* 67, 829–832 (1983).
- Langmead, B. & Salzberg, S.L. Fast gapped-read alignment with Bowtie 2. *Nat. Methods* 9, 357–359 (2012).
- Ogoshi, A. Ecology and Pathogenicity of anastomosis and intraspecific groups of *Rhizoctonia solani* Kuhn. *Annu. Rev. Phytopathol.* 25, 125–143 (1987).
- Shen, D., Ye, W., Dong, S., Wang, Y. & Dou, D. Characterization of intronic structures and alternative splicing in phytophthora sojae by comparative analysis of expressed sequence tags and genomic sequences. *Can. J. Microbiol.* 57, 84–90 (2011).
- Steele, L.D. *et al.* Genome-wide sequencing and an open reading frame analysis of dichlorodiphenyltrichloroethane (DDT) susceptible (91-C) and resistant (91-R) *Drosophila melanogaster* laboratory populations. *PLoS One* 9, e98584 (2014).
- Thorvaldsdóttir, H., Robinson, J.T. & Mesirov, J.P. Integrative genomics viewer (IGV): High-performance genomics data visualization and exploration. *Brief. Bioinform.* 14, 178–192 (2013).
- Trapnell, C. *et al.* Differential gene and transcript expression analysis of RNA-seq experiments with TopHat and Cufflinks. *Nat. Protoc.* 7, 562–578 (2012).
- Wibberg, D. *et al.* Draft genome sequence of the potato pathogen *Rhizoctonia solani* AG3-PT isolate Ben3. *Arch. Microbiol.* 199, 1065–1068 (2017).
- Wibberg, D. *et al.* Genome analysis of the sugar beet pathogen *Rhizoctonia solani* AG2-2IIIB revealed high numbers in secreted proteins and cell wall degrading enzymes. *BMC Genomics* 17, 245 (2016).
- Yamamoto, N. *et al.* Integrative transcriptome analysis discloses the molecular basis of a heterogeneous fungal phytopathogen complex, *Rhizoctonia solani* AG-1 subgroups. *Sci. Rep.* 9, 19626 (2019).

- Zhang, C., Gschwend, A.R., Ouyang, Y. & Long, M. Evolution of gene structural complexity: An alternative-splicing-based model accounts for intron-containing retrogenes. *Plant Physiol.* 165, 412–423 (2014).
- Zhao, C., Waalwijk, C., de Wit, P.J.G.M., Tang, D. & van der Lee, T. RNA-Seq analysis reveals new gene models and alternative splicing in the fungal pathogen *Fusarium graminearum*. *BMC Genomics* 14, 21 (2013).
- Zheng, A. *et al.* The evolution and pathogenic mechanisms of the rice sheath blight pathogen. *Nat. Commun.* 4, 1424 (2013).

Chapter 5

Expression profiles and functional analysis of *RsSEPGs* during infection

Abstract

Plants are equipped with a robust immune system by which they can suppress pathogen's invasion. Plant pathogens use effector proteins to suppress plant defenses and invade plant tissue. Effectors are differentially expressed during pathogen infection. Phytopathogens are varied in their lifestyle; effectors reported to be tightly regulated over the infection course. Pathogens express the effectors in-phase and tissue-specific manner. The infection strategy of the necrotrophic pathogen *Rhizoctonia solani* remains elusive. A recent report stated that *Brachypodium distachyon* accessions could induce a type of resistance against *R. solani*, mainly acting against biotrophic pathogens. Therefore, this pathogen should use effector protein to suppress plant immunity in a short biotrophic phase in its early infection stage. To identify *R. solani* secretory effector-like protein genes (*RsSEPGs*) expressed at the early infection process, the developed inoculation method using *B. distachyon* infected with *R. solani* was used. In this method, an increased amount of semi-synchronous infection hyphae is expected to be sampled from this approach. Therefore some effectors are expected to be detected earlier than before. Expression of *RsSEPGs* was analyzed at 6, 10, 16, 24, and 32 hours after inoculation by quantitative reverse transcription-polymerase chain reaction (qRT-PCR), out of 61 sequences validated genes; 52 genes could be detected in at least one-time point tested. Their expressions showed phase-specific patterns that were grouped into 6 clusters based on K-means clustering method. The 23 *RsSEPGs* in the cluster 1–3 and 29 *RsSEPGs* in the cluster 4–6 are expected to be involved in biotrophic and necrotrophic interactions, respectively. To get an insight into the necrosis inducing effector, transient expression of the *RsSEPGs* expressed in the later stage was conducted. The open reading frame of each gene was amplified and sub-cloned into *Agrobacterium tumefaciens*. Three genes were successfully evaluated and induce variable necrotic symptoms in the agro-infiltrated *Nicotiana benthamiana* leaves. Therefore, thesis findings provide a foundation for further functional analysis of the potential *RsSEPGs* expressed in early and late infection stages.

Introduction

Plant pathogens have developed sophisticated mechanisms to penetrate the plant cell wall for invasive growth. Production of a wide range of bioactive molecules such as enzymes, proteins, peptides, secondary metabolites, effectors, and toxins are crucial chemical tools for the successful invasion of host plants (Agrios 2005, Vincent *et al.* 2020). Plant pathogens are categorized as biotroph, hemibiotroph, and necrotroph with their nutrition acquisition manners (Glazebrook 2005). Biotrophs skim nutrients from living host cells, whereas necrotrophs kill the host cell before or during infection and obtain nutrients from decayed tissues. Hemibiotrophs go over as biotrophs during the early infection phase and shift to necrotrophic style later. Necrotrophs are subdivided into host-specific species and wide host-range species. In the interaction between host and biotrophic fungal pathogens, secretory effector proteins play a pivotal role in keeping down host immunity (Selin *et al.* 2016). They are loaded into apoplastic space, and some of them are incorporated into the host cell to target plant machinery for enemy sensing and defense execution in plants (de Jonge *et al.* 2011). In the studies of necrotrophic pathogens, necrosis-inducing factors including toxins and cell-wall-degrading enzymes have been in the spotlight intensively as important virulence factors. While small-secreted proteins and secondary metabolites with host-specific phytotoxic activities, so-called necrotrophic effectors have been identified as a critical determinant of pathogenicity of host-selective necrotrophs (Tan *et al.* 2010, Wang *et al.* 2014).

Rhizoctonia solani is a necrotrophic pathogen and its infection behaviour on the infected rice and *B. distachyon* has been studied (Zheng *et al.* 2013, Kouzai *et al.* 2018a). It was found that foliar treatment of salicylic acid (SA) conferred resistance to sheath blight disease caused by this pathogen in rice and *B. distachyon* (Kouzai *et al.* 2018a, Kouzai *et al.* 2018b). As a similar observation, exogenous application of benzothiadiazole (BTH), a functional SA analogue, was reported to increase resistance in *Brassica napus* to *Sclerotinia sclerotium*, an ascomycetous necrotrophic pathogen (Nováková *et al.* 2014). These results suggest that they may go through a short biotrophic phase in its infection process, which is effectively blocked by the SA-dependent host defense (Glazebrook 2005). Consistent with this scenario, three accessions Bd3-1, Gaz-4, and Tek-3 of *B. distachyon* showed disease resistance against *R. solani* (Kouzai *et al.* 2018a, Kouzai *et al.* 2020). Because these resistance accessions quickly induced SA-dependent marker genes after inoculation, they may recognize pathogen-derived molecules, probably effector proteins as an avirulent factor, for the induction of disease resistance response, as is the case in *V. dahlia* (Kawchuk *et al.* 2001, de Jonge *et al.* 2011).

Taken together, *R. solani* is likely to employ effector proteins for not only pursuance of necrosis at the later infection stage but also suppression of host immunity at the early infection stage.

Over the years, efforts to understand the plant-pathogen interaction have been accomplished using omics approaches (Witzel *et al.* 2015). Recent genomic studies have shown great diversity in genes related to pathogenicity in plant pathogens. A plethora of secretory protein genes as potential virulence factors have been identified from the genome of *R. solani* (Zheng *et al.* 2013). Several carbohydrate-active enzymes (CAZyme) genes and secreted effector proteins were identified during *Rhizoctonia*-Rice interaction. Common CAZyme gene families such as glycoside hydrolase (GH) and polysaccharide lyase (PL) were identified in the genome of *R. solani* (Zheng *et al.* 2013, Yamamoto *et al.* 2019).

Effectors are secreted protein involved in manipulating plant immunity for successful infection (Jones and Dangl 2006). A set of conserved effectors which has a significant contribution to pathogen virulence has been reported. NIS1 is a core effector protein from *Colletotrichum spp* found to suppress the hypersensitive response and oxidative burst induced by PAMPs in *Nicotiana benthamiana* (Irieda *et al.* 2018). The conserved secreted effector protein CfEC92 from *C. fructicola* can promote early appressorial penetration of apple leaves by suppressing PTI responses (Shang *et al.* 2020). The LysM-containing effectors were involved in scavenging some PAMPs, preventing them from induction of plant immunity. The LysM effector RsLysM from *R. solani* and SIP1 from *Magnaporthe oryzae* binds to chitin fragments released from the fungal cell wall. Therefore, it competes with chitin PRR-binding protein and eventually suppresses chitin-triggered immunity (Zhang and Xu 2014, Dolfors *et al.* 2019).

To counteract pathogens that use effectors to suppress host immunity, plants have the capability to recognize effector proteins directly or indirectly and activated the Effector Triggered Immunity (ETI) which can prevent pathogen progression (Jones and Dangl 2006). PrtToxA is a small secreted protein required for pathogenicity in *Pyrenophora tritici-repentis*, a causal agent of tan spot disease of wheat (Balance *et al.* 1989, Tuori *et al.* 1995, Tomas *et al.* 1990). The virulence function of these proteins needs *Tsn1*, which encodes the nucleotide-binding site (NBS)-leucine rich repeat (LRR)-type disease resistance (R) protein. Programmed cell death as part of hypersensitive response (HR) triggered by the recognition of pathogen-derived effector protein facilitates infection of these necrotrophic pathogens (Faris *et al.* 2010). These cases are similar to the mode of action of a host-specific toxin victorin in necrotrophic fungus *Cochliobolus victoriae*, the causal agent of victoria blight disease of oat. It is indirectly

recognized by LOV1 NBS-LRR-type R protein through thioredoxin-h5 in the host and induces disease resistance response, which makes the host susceptible (Lorang *et al.* 2007, Lorang *et al.* 2012).

To address the knowledge gap in the early expressed effector proteins secreted by *R. solani*, effector candidate genes were surveyed in this study. The improved inoculation method described in chapter 2 was used to analyze the expression of the potential predicted *RsSEPGs* listed in chapter 3. Using the qRT-PCR, I investigated the expression of 51 *RsSEPGs* during the infection in *B. distachyon*. They were finally classified into 6 clusters with their expression timing and 23 and 29 genes were detected at earlier and later time points, respectively. The expression of 22 *RsSEPGs* could be newly characterized in this study. Because the 29 genes were expected to have a function in necrosis induction, their possible necrosis induction activities were verified using the Agrobacterium-mediated transient expression method in *B. distachyon* as well as *N. benthamiana*. Variable necrosis symptoms were observed by three genes (*AG1IA_02940*, *AG1IA_08487*, and *AG1IA_07047*) in *N. benthamiana*.

Materials and Methods

Plant and fungal materials

This is described in chapter 2.

RNA-seq analysis

This is described in chapter 2.

Inoculation test

This is described in chapter 2.

Gene expression analysis

This is described in chapter 2.

Z-scaling and k-means clustering of expression profiles of *RsSEPGs*

The expression level of each *RsSEPG* normalized with *18S rRNA* gene during infection was converted to z-scores using *genescale* function in *genefilter* of Bioconductor R package (Gentleman *et al.* 2004). The z-scaling expression profiles were classified into 6 clusters with k-means algorithm using Multi Experiment Viewer (MeV) (Saeed *et al.* 2006).

Plasmid construction of *RsSEPGs* expressed in the necrotrophic stage

The total RNA harvested from the inoculated leaves at 24hpi was used to synthesize the complementary DNA using the PrimeScript RT reagent Kit with gDNA Eraser (Takara Bio). The coding sequence of each *RsSEPGs* was amplified using a specific PCR primer (Table 8) designed by Primer3 an online software tool (Untergasser *et al.* 2012) and cloned into pENTRTM/D-TOPO[®] vector (Invitrogen) according to the manufacturer instructions. pENTRTM/D-TOPO[®] vector was transformed into *E. coli* strain DH5 α TM (Promega) (Appendix A). Transformed bacterial cells were grown on the Luria-Bertani Agar (LBA) medium supplemented with Kanamycin sulfate (50 μ g/ml) and incubate at 37 °C overnight. Growing colonies were selected by colony PCR followed by electrophoresis. Colonies with correct insert size were grown on Luria-Bertani Broth (LBB) medium supplemented with Kanamycin sulfate (50 μ g/ml) and incubate at 37 °C with shaking overnight. Then plasmid was extracted using FastGene[®] Plasmid Mini Kit (NIPPON GENETICS) according to the manufacturer instructions. The extracted plasmids' quality and quantity were checked using DS-11 Spectrophotometer (DeNovix). Followed by sequence analysis, insert in the sequence-validated vector was shuttled into the pGWB2 destination vector *via* LR reaction according to the manufacturer instructions (Invitrogen) (Appendix A).

Transient Expression of *RsSEPGs* in *B. dystachyon*, *A. thaliana* and *N. benthamiana*

Using the electroporation method, the constructed pGWB2 destination vectors for each gene were transformed into the electrocompetent *Agrobacterium* strains EHA105 and GV3101 according to Kaman-Toth *et al.* 2018. *Agrobacterium* strains harboring pGWB2 were grown on LBA medium supplemented with Kanamycin sulfate and Hygromycin B (50 µg/ml) (Appendix B). Correct clones were selected by colony PCR followed by electrophoresis. Colonies with correct insert size were grown on liquid LBB medium supplemented with Kanamycin sulfate (50 µg/ml) and Hygromycin B (50 µg/ml) overnight with rotation at 160 rpm at 28 °C. Aliquots of 400 µL inoculated to 10 mL of a fresh liquid LBB medium supplemented with kanamycin (50 µg/L) and Hygromycin (50 µg/L) with rotation at 160 rpm at 27 °C for 24h. *Agrobacterium* cells were collected by centrifugation at 4,000 x g for 10 min and suspended in infiltration buffer (10 mM MES pH = 5.6, 10 mM MgCl₂, 0.03% Tween20, 200 µM acetosyringone) to an optical cell density of 1 at 600 for *B. dystachyon*, and to an OD 0.6 for *N. benthamiana* then incubated for 3h prior infiltration according to Bashandy *et al.* 2015. Leaves of four-week-old *N. benthamiana* were infiltrated with *Agrobacterium* strain GV3101 and three-week-old *B. dystachyon* were infiltrated with EHA105 using needleless syringes. Leaves were subsequently observed for symptoms and photographed.

Semi-quantitative RT-PCR

To confirm the transformation efficiency and the expression of *RsSEPGs* after agro-infiltration; *N. benthamiana* leaves samples from the infiltrated plants were collected at 2dpi and 6dpi; then total RNAs were extracted using ISOSPIN Plant RNA extraction Kit (NIPPON GENE CO., LTD. Tokyo, Japan). Concentration and purity of extracted RNAs were checked using DS-11 Spectrophotometer (DeNovix). cDNAs were synthesized using PrimeScript RT reagent Kit with gDNA Eraser (Takara Bio). The Actin gene from *N. benthamiana* was used as an internal control (Cheng *et al.* 2013). GoTaq® G2 Hot Start Green Master Mix (Promega) and T100 thermal cycler (Bio-Rad, Hercules, CA, USA) was used for qRT-PCR analysis. Reactions were analyzed by gel electrophoresis.

Results

Analysis of transcriptions of *RsSEPGs* during infection in *B. distachyon*

To analyze expression levels of the 61 *RsSEPGs* selected after calibration of their gene model by qRT-PCR, specific primers for each gene were designed (Table 6). Note that annotated gene models were used for primer design in 13 *RsSEPGs* whose RNA-sequencing reads were not observed in our sample. Expression levels of *RsSEPGs* were determined as an average of 4 biological replicates (Figures. 4, 5, and 6). Transcripts of 52 *RsSEPGs* but not the others could be detected at least at a single time point tested in our experimental condition. We performed this experiment twice and similar expression patterns could be observed except 6 genes *AGIIA_00431*, *AGIIA_03254*, *AGIIA_08487*, *AGIIA_08650*, *AGIIA_09956*, and *AGIIA_10146*, which demonstrated different expression patterns (Figure 4).

Expressions of 9 *RsSEPGs* were not detected in this study and their transcripts were also almost undetected in PDA medium-grown hyphae analyzed by RNA-seq. On the contrary, 9 genes were expressed during infection although they were not transcribed on PDA medium (FPKM <1) (Table 7).

Table 6. Gene ID and primer list used for qRT-PCR

| Gene ID | Primer sequence | Gene | Primer sequence |
|-------------|---------------------------|-------------|--------------------------|
| AG11A_00157 | CCCATGCTCACTTGGCTTC | AG11A_06710 | GATACGGCTCGAAGCAACTAAG |
| | CCCTTACTTCGTCATCATACTCACC | | GGTTTTACTCGCCACTGCTTG |
| AG11A_00273 | CCGCAATGCAAGTCAAAGG | AG11A_06739 | CGCCTCTGGTGGTCTCTACTACTC |
| | GCAAAGGGACGAAGGTGTG | | GAAATCCGAAATGATTGCCTTG |
| AG11A_00431 | GGGATCGACTGGGATAAAAAGTG | AG11A_07047 | CGGTTGCTATCTGCCTTCC |
| | ATCGCACCTTGCCGTTG | | GTAGTCTTCCCGTCCCATCC |
| AG11A_00478 | GGGTTGACGAGTTTGCCTTC | AG11A_07075 | CCGATTGCCGTTGGAAG |
| | TAATAGCGTGGTCCGTTCTTCC | | AGTAGAATACACCTGGGCGAAAAC |
| AG11A_00669 | TGTTCTCTTCGCTGTATCGTTTG | AG11A_07122 | TCTCTAGTCAGCCGCCCATC |
| | ACGACGGATTGGAGACTTGG | | GATTTGTTCTCTGGTTTCGAGGTC |
| AG11A_00684 | GGCAAGTTCCAAGGGAGTG | AG11A_07262 | TTGATCTTGTGCTCTGCCATC |
| | AAATCCAACGACCCGAGAAG | | CTTTCCTCCGCATTACACC |
| AG11A_00763 | TGGGAGAAAGGGACAGCAAG | AG11A_07267 | GTCGACTGGCTCACACCTTC |
| | ACAGTGATTTGCCTCGTTCG | | ACGCACTAAACAGCGCAAAC |
| AG11A_00879 | TGACTGAGATGGAGAAATCACAC | AG11A_07958 | GCGATCAATATCAACGACCAAG |
| | TTCTGGTAGCCTGTAATCGTAATC | | TGAGAGGGAGTATGACGGAGTG |
| AG11A_00951 | GGCCGATGTCGAGAACTTG | AG11A_07966 | GATCCATGCTATGCCAGTACCTC |
| | TACACCGCAGGGTCTTTG | | GTCGCCATCCACAACCATC |
| AG11A_01042 | CATCTGGGATTGACGCTTATGTC | AG11A_08025 | GACTCTTGAACCACAGTCTCC |
| | TTCTGCTGCCGATTTC | | TTCTCTGCCTTTCGTATCC |
| AG11A_01512 | GGCCTCAGGAAGACACAAGG | AG11A_08061 | GGTCGCAGTTTCATCATCTCC |
| | TGGAAGGGATAGGTGGGAAAC | | TTGCGGCGAATCCAAAG |
| AG11A_01603 | CTAAATTGGTTGTGCTG | AG11A_08487 | CACGTTTTCAATAACAGGGAAGG |
| | CGCTCTCGTGTATCGCATTTAC | | TAAACCGACGAGCGGAAAAG |
| AG11A_01604 | CGAAGGCAGATGCGATACAC | AG11A_08488 | CTTTGTTGAGTTCCCTATTTTCC |
| | TCATAGTCCGAAGTCCAAGTCC | | AGCCCTTATACTGCCGATG |
| AG11A_01605 | CGCTTCGCTTATTGATTGCTC | AG11A_08577 | CTTGCTTGTGCCCTAATACGACTG |
| | GGGTCGGTTGTCGCTTTAC | | TTTGACGGGTGGCTTG |
| AG11A_01933 | AGGCACCGCTAATTGTTG | AG11A_08615 | CCCTCTTGAATCAACGTCTTGG |
| | CCAGACGATCCAAATCAACTC | | CTACTGCCTCTGTTCATCTGG |
| AG11A_02940 | AACACATCGCTCTTGGATATGG | AG11A_08650 | TTTACGACCAACCCGCCTAC |
| | TTCTGGGTCGGTTTGGTG | | CCTGGTTAAGTCCAGCCAACCTC |
| AG11A_03047 | GACCATTCCAAGACGACCAG | AG11A_08777 | CCAAGGAATCAGGAGGAAAGTG |
| | GGGAATCGGGATAATGCAAG | | TCCAAAAGGGTCCCGTGAATG |
| AG11A_03254 | GAAAGGCACGGATAGGAAAGG | AG11A_09055 | TGCGAATGTAGTCGCTCACC |
| | GCCGAGTACGGTAACAAAAGG | | TAAACCCGCCAACCAAACCTC |
| AG11A_04006 | TTCTGTCGGCTTGTTCG | AG11A_09060 | CGCCTGTCCATTACCATC |
| | ACACGGGTGAAGAGACAGG | | CCAAATACGACCAGCCTTCC |
| AG11A_04237 | GCCCCAGTATCTCTGTTTGTG | AG11A_09202 | AGGCTTCTGCTCGCCTTC |
| | CACAATGACCTCCAAAATCTTCC | | GTTGCCACTCCCTCCACTACC |
| AG11A_04298 | GTCGTAGACAGATCAGAACACCAAC | AG11A_09203 | GCCTTTGCTTCCCCTCTTG |
| | CGAAATAACACTCCCACCAAG | | GTAAGATTGCATTTGCCCTTCC |
| AG11A_04737 | AGCGTGGTGAAGCGAATG | AG11A_09207 | GTGGAATGCCGCTGACTG |
| | CAGACGGATGGCTGTAACGTAG | | CGTATTTCCGCCCTTCTTG |
| AG11A_04814 | CATAGGAAACGCTCGGCAAC | AG11A_09229 | GGCTCCACCCAGAGCATAAATAC |
| | TGGCACTGATGAGACGGTAGAG | | CGCATTACCTCTCGCCTAC |
| AG11A_04819 | CCGTCAGTTTCGIGTAATCACTATG | AG11A_09643 | TTTTGTGATTCTGGCTGTGTAG |
| | AGATGTGATTGTGGTGGTTGATG | | CAGACCGCACAGGTCTCTAAC |
| AG11A_05291 | GCGCGGCTGTTTCTTG | AG11A_09728 | TGGCCGGACCAACAATAAG |
| | GACACGAGAGTTGGCAATG | | CGAGAAAAGCTCATAGAAACAATC |
| AG11A_05500 | GGACTGCTGCATTAAGGTTGG | AG11A_09837 | AAGGTGGTGGCAGTAACG |
| | GCACGATGGCTGGTTGTAAG | | GGATGAACAACACCCTGATCC |
| AG11A_05783 | CCGAGCCGAGAAGATCAAG | AG11A_09956 | TAGCAGAGATTGCTGCACAAGAG |
| | AGTTATTGGTCAAGTCAAGGAAG | | ACGGCAACACTCCTTGTATCTTC |
| AG11A_05938 | CAAGAGCAAACGACCCGATG | AG11A_10146 | TTTCGTCGCTGCCAAG |
| | GCCAAGTCCAACAGCAAG | | CCTGGAAGAGGTGAGCCAAG |
| AG11A_06169 | GACAATCAGGACGACAACGAG | AG11A_10284 | ATCCGCCACCTCTGTTAGC |
| | ATTGCAGACTTTAGCGAACCAAG | | CAGGTGCTGGCGATACAAC |
| AG11A_06325 | GTGTGTTGGTGAAGCGAAAAG | AG11A_10478 | CGACTCCCTTGCCTATTTCTTG |
| | GGTCCCTGATGCCAATAGTTC | | CAAGTTTCTCCACTCCCTACGAAC |
| AG11A_06613 | TTGTTGTCGTTGCTGCTCTTG | 18S rRNA | AATTCCAGCTCAATAGCGT |
| | CTGCCTTCCGTTGATACCC | | TACATACCGTGAGGCAGACC |

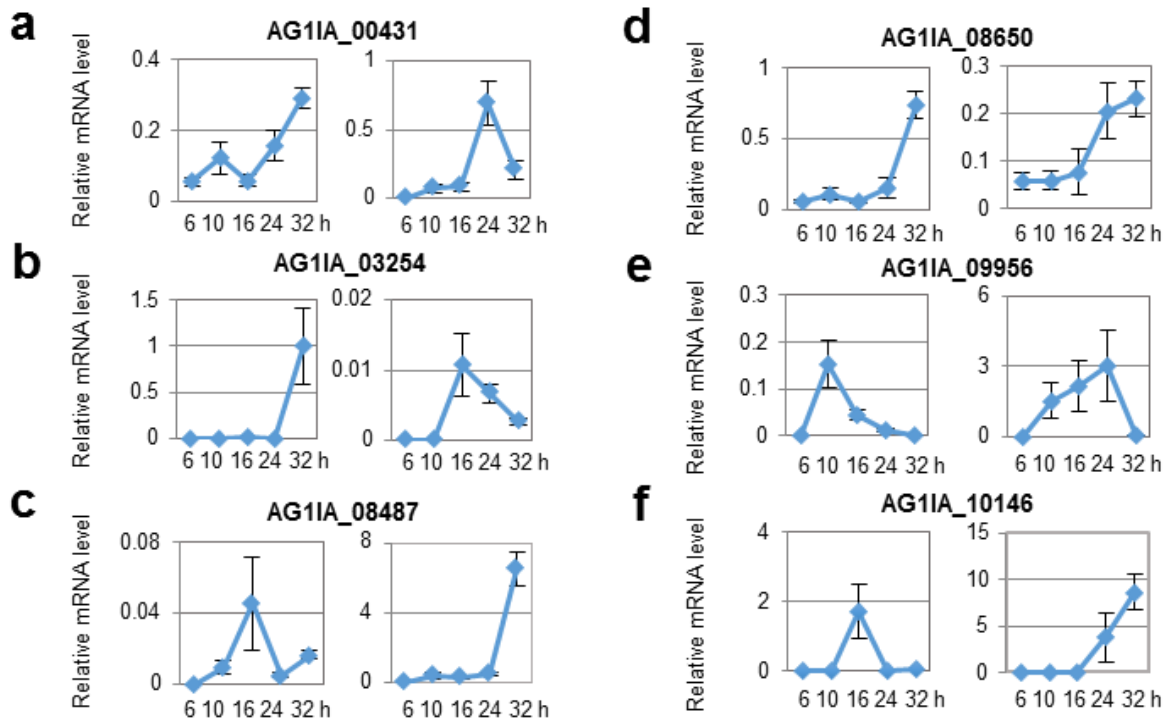


Figure 7. Expression profiles of *R*sSEPGs during the infection of *Rhizoctonia solani* on detached leaves of *Brachypodium distachyon* which showed different expression patterns in two independent experiments. (a to f) Expressions of *AG1IA_00431* (cluster 4 or 6) (a), *AG1IA_03254* (cluster 6 or 3) (b), *AG1IA_08487* (cluster 3 or 6) (c), *AG1IA_08650* (cluster 6 or 5) (d), *AG1IA_09956* (cluster 2 or 3) (e), and *AG1IA_10146* (cluster 3 or 6) (f) of *R. solani*, which were classified into different clusters with their expression patterns, on *B. distachyon* at 6, 10, 16, 24, and 32 hours post-inoculation with the improved method. Gene expressions were examined using qRT-PCR using cDNA prepared with total RNAs extracted from *R. solani*-inoculated *B. distachyon* leaves at each time point. Graphs display the relative mRNA level of each gene normalized by *18S rRNA* as the internal control. The data are presented as means with the standard error of 4 biological replicates. The results of two independent experiments were shown.

K-means clustering of gene expression patterns of *RsSEPGs*

RsSEPGs displayed variable expression patterns over the time course. To classify *RsSEPGs* with their expression patterns, we transformed the expression levels of each *RsSEPGs* during infection into z-scores as a method for standardization and normalization which represents the variation of relative expression levels. Then, they were depicted as a heatmap (Figure 5) (Cheadle *et al.* 2003). By using the k-means algorithm, the z-scaling expression profiles of 52 *RsSEPGs* could be classified into 6 clusters (Figure 5 and Table 7) (D'Haeseleer *et al.* 2005). Note that, for 6 genes with varied expression patterns in two independent experiments, every single result was used as a representative.

Cluster 1 includes 6 genes expressed with peaks at 6 hpi and then they were gradually decreased during infection. Cluster 2, 3, and 4 consist of 14, 3, and 9 genes, respectively, whose transcripts were predominantly accumulated at 10, 16, and 24 hpi. Transcriptions of 11 genes in cluster 5 were detected in both 24 and 32 hpi. Nine genes in cluster 6 predominantly expressed at 32 hpi. Because necrotic lesions appeared from 24 hpi in our inoculation system, the 23 *RsSEPGs* in the cluster 1, 2, and 3 are expected to have biological roles for the establishment of potential biotrophic invasion of *R. solani*. On the other hand, the remaining 29 genes in the other clusters may function mainly for the necrotic stage.

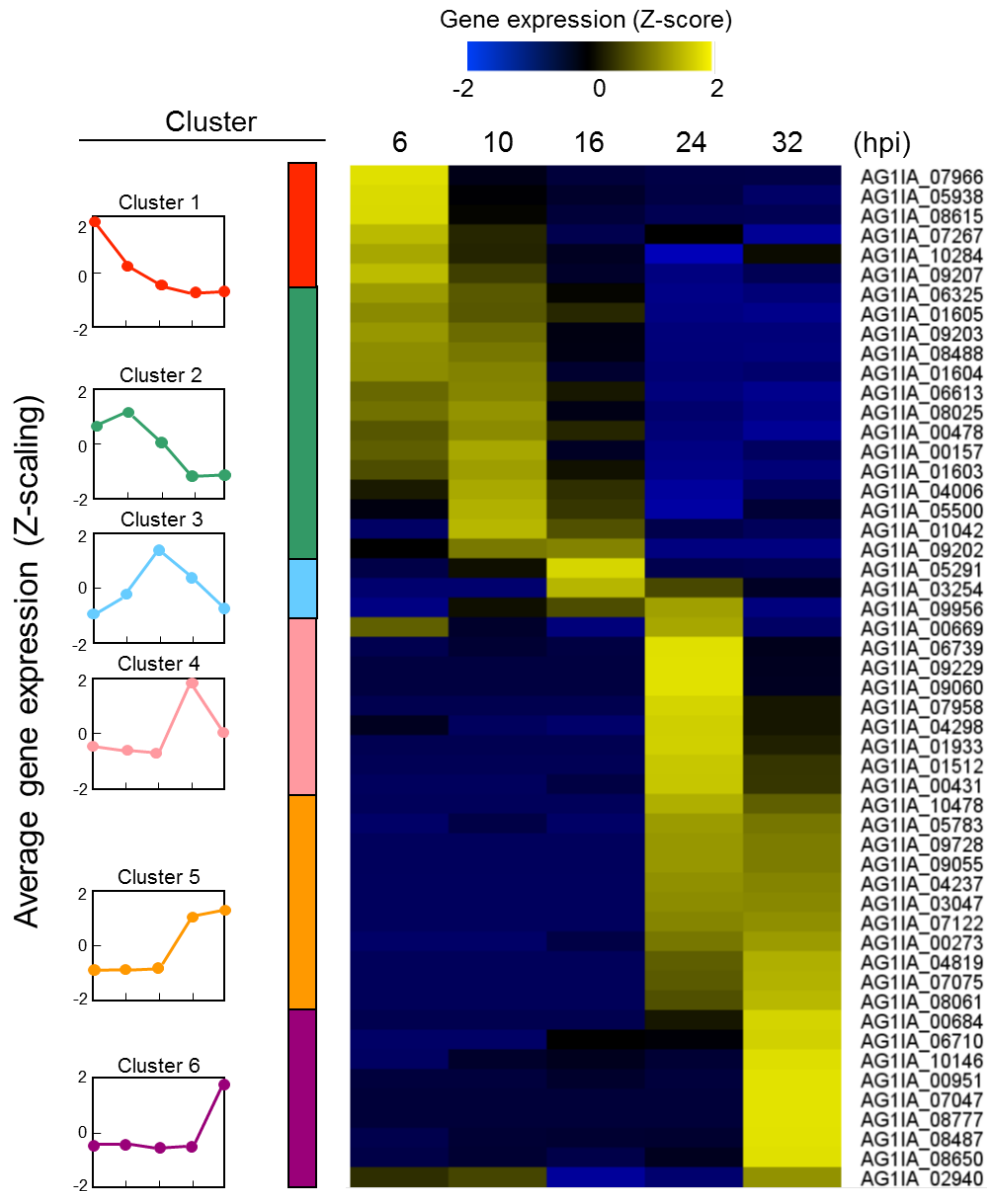


Figure 8. Expression dynamics of *R*sSEPGs during infection on *Brachypodium distachyon* and their clustering with expression patterns. Expression levels of each gene during infection (6–32 hours post-inoculation) were converted to z-scores and their values were represented as a heatmap. The time point with higher expression levels compared with the others in each gene is shown with yellow color. These *R*sSEPGs were classified into 6 categories with their expression patterns by the k-means clustering method. The average pattern of each cluster was depicted with colors on the left column.

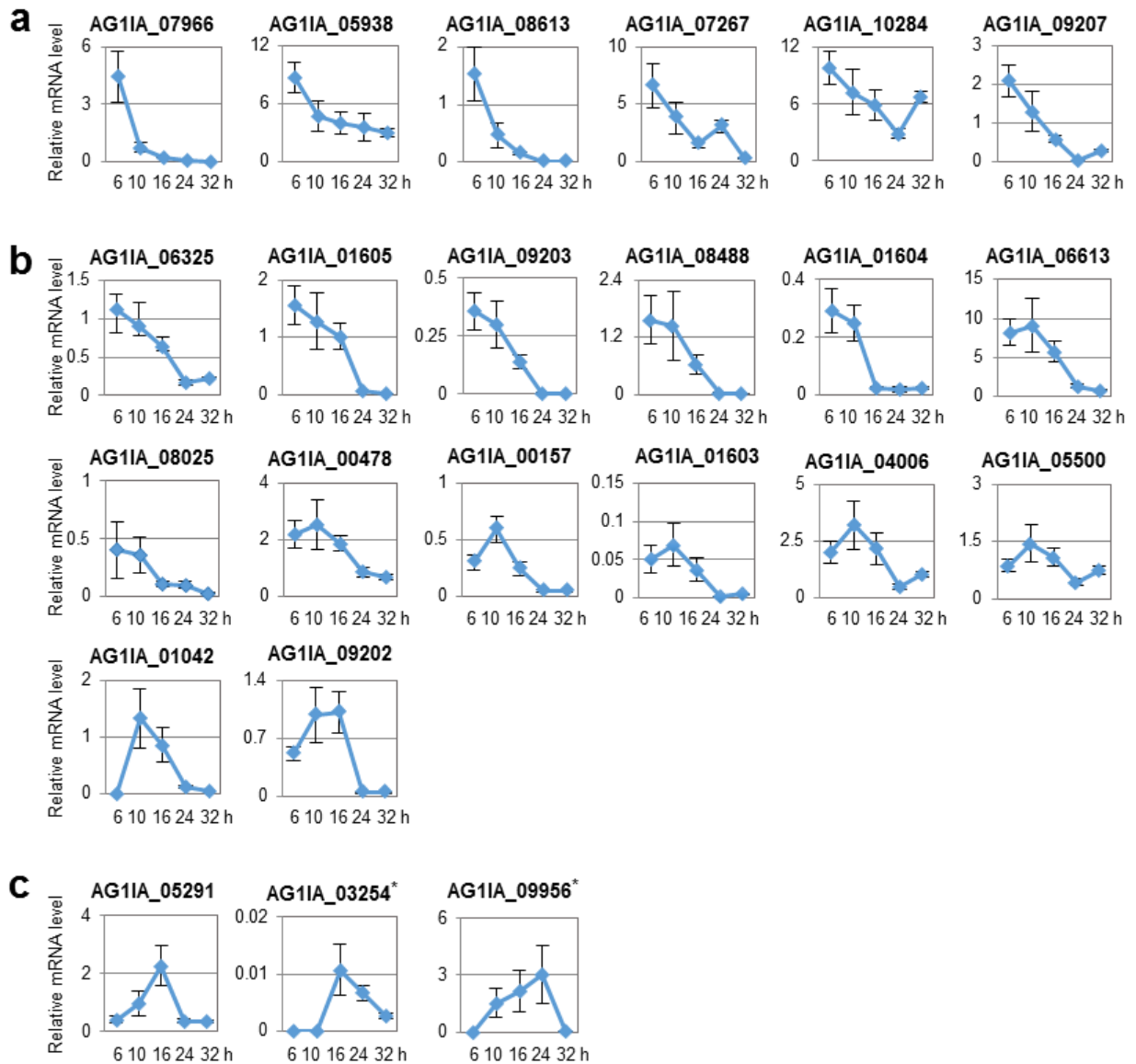


Figure 9. Expression profiles of *RsSEPGs* during *Rhizoctonia solani* infection on the detached leaves of *Brachypodium distachyon*. (a to c) Expression of 6, 14, and 3 *RsSEPGs* of *R. solani* categorized as cluster 1 (a), 2 (b), and 3 (c), respectively, on *B. distachyon* at 6, 10, 16, 24, and 32 hours post-inoculation with the improved inoculation method. Gene expressions were examined using qRT-PCR using cDNA prepared with total RNAs extracted from *R. solani*-inoculated *B. distachyon* leaves at each time point. Graphs display the relative mRNA level of each gene normalized by *18S rRNA* as an internal control. The data are presented as means with the standard error of 4 biological replicates. Experiments were performed twice with similar results except *AG1IA_03254* and *AG1IA_09956* marked with an asterisk and a representative result is shown.

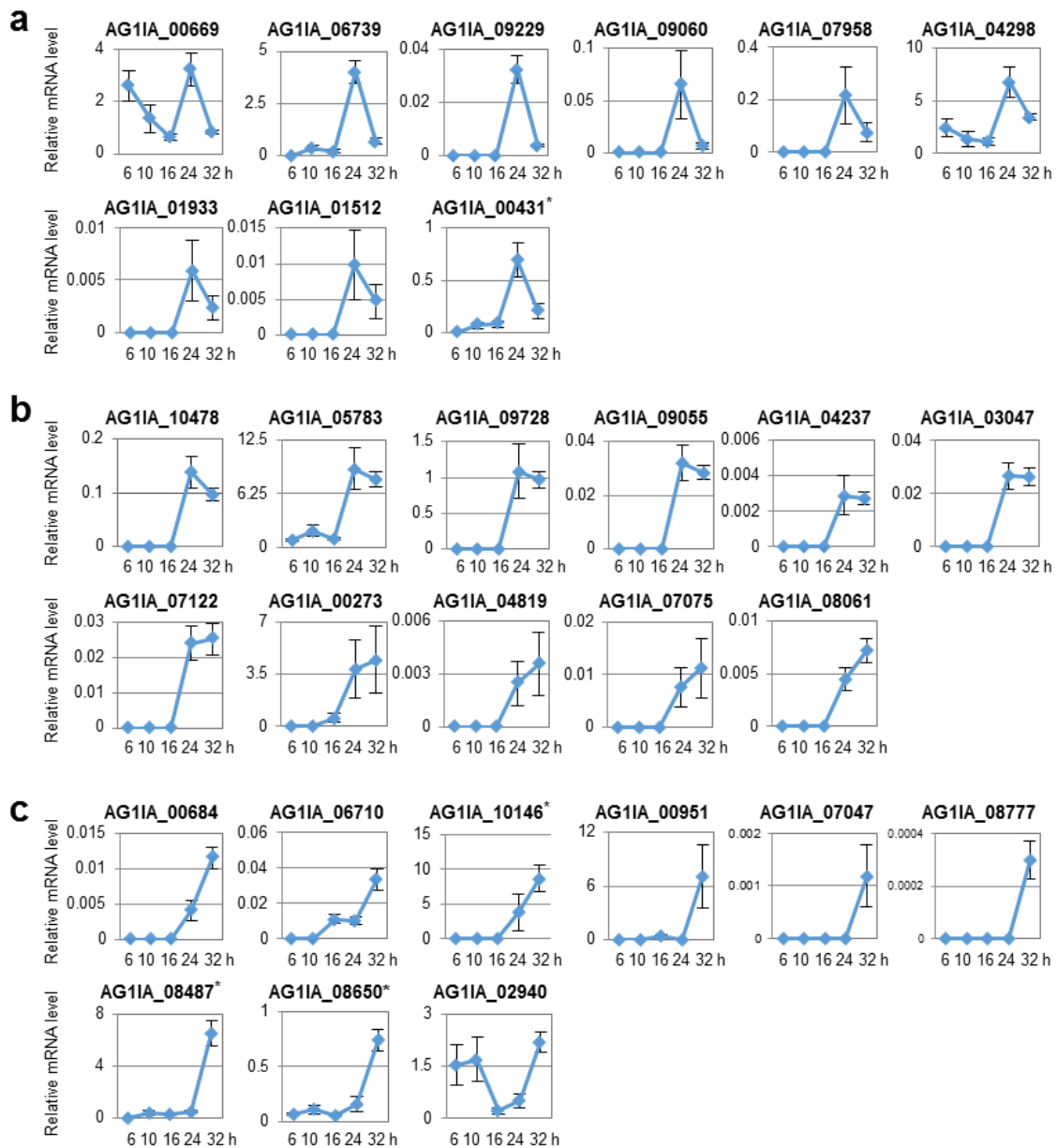


Figure 10. Expression profiles of *RsSEPGs* during *Rhizoctonia solani* infection on the detached leaves of *Brachypodium distachyon*. (**a** to **c**) Expression of 9, 11, and 9 *RsSEPGs* of *R. solani* categorized as cluster 4 (**a**), 5 (**b**), and 6 (**c**), respectively, on *B. distachyon* at 6, 10, 16, 24, and 32 hours post-inoculation with the improved method. Gene expressions were examined using qRT-PCR using cDNA prepared with total RNAs extracted from *R. solani* -inoculated *B. distachyon* leaves at each time point. Graphs display the relative mRNA level of each gene normalized by *18S rRNA* as an internal control. The data are presented as means with the standard error of 4 biological replicates. Experiments were performed twice with similar results except for *AG11A_00431*, *AG11A_08487*, *AG11A_08650*, and *AG11A_10146* marked with asterisks and a representative result is shown.

Comparison of the expression profiles of *RsSEPGs* with the previously characterized *R. solani* secretory genes on rice

Zheng *et al.* (2013) identified 965 potentially secreted proteins and 234 of them were demonstrated to show differential expression with 2-fold or greater during early infection progress at 10–24 hpi on rice. Among 61 *RsSEPGs* identified, 23 genes are found in the list of 234 genes. Thirteen of these shared genes (*AGIIA_00273*, *AGIIA_00684*, *AGIIA_03254*, *AGIIA_06739*, *AGIIA_07047*, *AGIIA_07958*, *AGIIA_07966*, *AGIIA_08061*, *AGIIA_04237*, *AGIIA_08487*, *AGIIA_08615*, *AGIIA_08650*, and *AGIIA_08777*) exhibited a better correlation with similar profiles in both studies (Table 6). However, the other 5 genes (*AGIIA_00157*, *AGIIA_00669*, *AGIIA_05291*, *AGIIA_08488*, and *AGIIA_09207*) showed varied expression patterns in both studies (Table 7). The expression of 9 *RsSEPGs* was not observed in our experimental condition, but 5 of them were detected in Zheng *et al.* (2013) (Table 7). While 34 out of 52 expressed *RsSEPGs* were undetected by Zheng *et al.* (2013), 13 of them were detected in the previous alternative transcriptome analysis by Xia *et al.* (2017). Thus, the expression patterns of 22 *RsSEPGs* were newly characterized in this study.

Table 7. *Rhizoctonia solani* AG-1 IA secretory effector protein genes (*RsSEPGs*) with their expressions during infection and agar medium

| GeneID | Cluster ^a | Expression timing in Zheng et al (2013) ^b | Detection of transcripts in Xia et al -2017 | Annotation ^c | Expression levels on PDA medium (FPKM) ^d | | | |
|--------------------|----------------------|--|---|---|---|--------|-------|------|
| | | | | | Rep1 | Rep2 | Rep3 | AVG |
| AG1IA_00153 | n.a. | 24 hpi | | hypothetical protein | 12.11 | 23.17 | 22.26 | 19.2 |
| AG1IA_00157 | 2 | 24 hpi | | polysaccharide deacetylase domain-containing protein | 4.51 | 7.52 | 9.41 | 7.15 |
| AG1IA_00172 | n.a. | n.a. | | Cysteine proteinase | 12.46 | 18.47 | 22.04 | 17.7 |
| AG1IA_00273 | 5 | 10, 18 hpi | yes | hypothetical protein | 92.34 | 48.5 | 32.69 | 57.8 |
| AG1IA_00431 | 4 or 6 | n.a. | | GILT domain-containing protein | 215.43 | 168.17 | 173.4 | 186 |
| AG1IA_00478 | 2 | n.a. | | hypothetical protein | 20.93 | 25.13 | 26.58 | 24.2 |
| AG1IA_00529 | n.a. | n.a. | | hypothetical protein | 8.07 | 6.39 | 7.29 | 7.25 |
| AG1IA_00669 | 4 | 10 hpi | | glycosyl hydrolase family 61 domain-containing protein | 91.92 | 140.04 | 126.4 | 119 |
| AG1IA_00684 | 6 | 10, 18 hpi | | hypothetical protein | 0.27 | 0.71 | 0.69 | 0.55 |
| AG1IA_00763 | n.d. | 24 hpi | | hypothetical protein | 1.3 | 0 | 0 | 0.43 |
| AG1IA_00879 | n.d. | 10 hpi | | hypothetical protein | 6.56 | 8.45 | 7.23 | 7.41 |
| AG1IA_00951 | 6 | n.a. | | deuterolysin metalloprotease (M35) family domain-containing protein | 3107.04 | 2100.5 | 1562 | 2256 |
| AG1IA_01042 | 2 | n.a. | yes | hypothetical protein | 13.98 | 8.07 | 9.42 | 10.5 |
| AG1IA_01512 | 4 | n.a. | yes | hypothetical protein | 19.66 | 17.26 | 16.02 | 17.7 |
| AG1IA_01599 | n.a. | n.a. | | lipoic acid synthase | 86.49 | 86.45 | 91.46 | 88.1 |
| AG1IA_01603 | 2 | n.a. | | DUF1524 domain containing-protein | 10.51 | 14.77 | 14.81 | 13.4 |
| AG1IA_01604 | 2 | n.a. | yes | DUF1524 domain containing-protein | 15.46 | 18 | 14.69 | 16.1 |
| AG1IA_01605 | 2 | n.a. | | hypothetical protein | 148.22 | 164.07 | 160 | 157 |
| AG1IA_01933 | 4 | n.a. | | hypothetical protein | 0.91 | 2.65 | 2.15 | 1.9 |
| AG1IA_02138 | n.a. | n.a. | | hypothetical protein | 58.78 | 74.98 | 67.94 | 67.2 |
| AG1IA_02490 | n.a. | n.a. | | hypothetical protein | 0.59 | 0 | 0 | 0.2 |
| AG1IA_02878/79/80 | n.a. | 24 hpi | | DNA binding domain-containing protein | 35.98 | 47.58 | 45.14 | 42.9 |
| AG1IA_02940 | 6 | n.a. | | DUF3455 domain containing-protein | 430.26 | 251.35 | 207.4 | 296 |
| AG1IA_03047 | 5 | n.a. | | hypothetical protein | 1.3 | 0.73 | 0 | 0.67 |
| AG1IA_03254 | 3 or 6 | 10 hpi | | hypothetical protein | 9.03 | 12.85 | 14.38 | 12.1 |
| AG1IA_04006 | 2 | n.a. | | hypothetical protein | 8.63 | 21.74 | 13 | 14.5 |
| AG1IA_04108 | n.a. | 24 hpi | | hypothetical protein | 2.12 | 4.91 | 6.18 | 4.4 |
| AG1IA_04191 | n.a. | 10 hpi | | hypothetical protein | 0.62 | 1 | 0.16 | 0.59 |
| AG1IA_04237 | 5 | 24 hpi | | hypothetical protein | 0.49 | 0.52 | 0.12 | 0.38 |
| AG1IA_04267/8 | n.a. | n.a. | | Viral tegment protein/pectinesterase inhibitor | 53.65 | 55.73 | 54.81 | 54.7 |
| AG1IA_04298 | 4 | n.a. | | emp24/gp25L/p24 family/GOLD domain-containing protein | 66.3 | 64.66 | 71.39 | 67.5 |
| AG1IA_04737 | n.d. | n.a. | | hypothetical protein | 0 | 0 | 0 | 0 |
| AG1IA_04814 | n.d. | 10 hpi | | hypothetical protein | 0.22 | 0.36 | 0.23 | 0.27 |
| AG1IA_04819 | 5 | n.a. | | fungal cellulose binding domain-containing protein | 0 | 0 | 0 | 0 |
| AG1IA_04889 | n.a. | n.a. | | hypothetical protein | 0 | 0 | 0 | 0 |
| AG1IA_05179 | n.a. | n.a. | Yes | hypothetical protein | 0.13 | 0.29 | 0 | 0.14 |
| AG1IA_05291 | 3 | 24 hpi | Yes | hypothetical protein | 35.87 | 41.33 | 33.47 | 36.9 |
| AG1IA_05500 | 2 | n.a. | | hypothetical protein | 780.36 | 928.89 | 845.6 | 852 |
| AG1IA_05601 | n.a. | 24 hpi | | histone acetyl transferase | 15.28 | 11.79 | 19.81 | 15.6 |
| AG1IA_05783 | 5 | n.a. | | hypothetical protein | 27.82 | 56.66 | 58.08 | 47.5 |
| AG1IA_05938 | 1 | n.a. | | hypothetical protein | 28.44 | 78.85 | 63.3 | 56.9 |
| AG1IA_06169 | n.d. | 24 hpi | | hypothetical protein | 0 | 0 | 0 | 0 |
| AG1IA_06325 | 2 | n.a. | Yes | FKBP-type peptidyl-prolyl cis-trans isomerase domain-containing protein | 149.73 | 212.66 | 194.4 | 186 |
| AG1IA_06613 | 2 | n.a. | Yes | DUF3129 domain containing-protein | 183.12 | 312.28 | 273.8 | 256 |

Table 7. continued. *Rhizoctonia solani* AG-1 IA secretory effector protein genes (*RsSEPGs*) with their expressions during infection and agar medium

| GeneID | Cluster a | Expression timing in Zheng et al (2013) b | Detection of transcripts in Xia et al -2017 | Annotation c | Expression levels on PDA medium (FPKM) d | | | |
|-------------|-----------|---|---|---|--|-------|--------|-------|
| | | | | | Rep1 | Rep2 | Rep3 | AVG |
| AG1IA_06710 | 6 | n.a. | | hypothetical protein | 0 | 0.63 | 0.4 | 0.34 |
| AG1IA_06739 | 4 | 18, 24 hpi | | hypothetical protein | 9.26 | 7.92 | 9.28 | 8.82 |
| AG1IA_06741 | n.a. | 18, 24 hpi | | hypothetical protein | 1.26 | 0 | 1.68 | 0.98 |
| AG1IA_07047 | 6 | 24 hpi | | hypothetical protein | 31.69 | 30.05 | 25.03 | 28.92 |
| AG1IA_07075 | 5 | n.a. | yes | CFEM domain-containing protein | 1.57 | 4.68 | 3.22 | 3.15 |
| AG1IA_07122 | 5 | n.a. | | hypothetical protein | 0 | 0 | 0 | 0 |
| AG1IA_07262 | n.d. | n.a. | yes | hypothetical protein | 0.25 | 0.1 | 0.2 | 0.18 |
| AG1IA_07267 | 1 | n.a. | yes | hypothetical protein | 5.8 | 6.46 | 8.31 | 6.86 |
| AG1IA_07490 | n.a. | n.a. | | Yippee domain-containing protein | 10.59 | 10.34 | 12.1 | 11.01 |
| AG1IA_07958 | 4 | 18, 24 hpi | | igA peptidase M64 domain-containing protein | 13.85 | 10.61 | 12.07 | 12.18 |
| AG1IA_07966 | 1 | 10 hpi | | hypothetical protein | 8.19 | 9.09 | 9.3 | 8.86 |
| AG1IA_08025 | 2 | n.a. | | DUF3421 domain containing-protein | 38.43 | 44.08 | 37.76 | 40.09 |
| AG1IA_08061 | 5 | 10, 18 hpi | | hypothetical protein | 0.23 | 0.57 | 0.08 | 0.3 |
| AG1IA_08487 | 3 or 6 | 24 hpi | | Ribonuclease domain-containing protein | 384.71 | 416.2 | 430.21 | 410.4 |
| AG1IA_08488 | 2 | 24 hpi | yes | Ribonuclease domain-containing protein | 2.28 | 3.45 | 0.98 | 2.24 |
| AG1IA_08577 | n.d. | n.a. | | hypothetical protein | 0 | 0 | 0 | 0 |
| AG1IA_08615 | 1 | 10 hpi | yes | hypothetical protein | 24.78 | 25.15 | 25.99 | 25.31 |
| AG1IA_08650 | 5 or 6 | 24 hpi | | hypothetical protein | 23.9 | 58.04 | 48.62 | 43.52 |
| AG1IA_08777 | 6 | 24 hpi | | plastocyanin-like domain-containing protein | 0.48 | 0.72 | 0.77 | 0.65 |
| AG1IA_08781 | n.a. | 18, 24 hpi | | Cuticle-degrading protease | 61.13 | 42.02 | 19.48 | 40.87 |
| AG1IA_08891 | n.a. | n.a. | yes | hypothetical protein | 59.57 | 47.9 | 41.5 | 49.65 |
| AG1IA_08892 | n.a. | n.a. | yes | hypothetical protein | 63.82 | 47.94 | 45.15 | 52.3 |
| AG1IA_08957 | n.a. | n.a. | | hypothetical protein | 0 | 0 | 0 | 0 |
| AG1IA_09055 | 5 | n.a. | yes | thaumatin-like protein | 2.67 | 2.82 | 2.26 | 2.58 |
| AG1IA_09060 | 4 | n.a. | yes | thaumatin-like protein | 5.5 | 6.78 | 5.84 | 6.04 |
| AG1IA_09137 | n.a. | n.a. | | hypothetical protein | 5.06 | 2.22 | 3.63 | 3.64 |
| AG1IA_09202 | 2 | n.a. | yes | hypothetical protein | 106.32 | 205.4 | 185.35 | 165.7 |
| AG1IA_09203 | 2 | n.a. | yes | hypothetical protein | 38.83 | 52.21 | 43.66 | 44.9 |
| AG1IA_09207 | 1 | 24 hpi | yes | hypothetical protein | 316.59 | 322.3 | 235 | 291.3 |
| AG1IA_09229 | 4 | n.a. | | hypothetical protein | 2.5 | 1.32 | 1.04 | 1.62 |
| AG1IA_09275 | n.a. | n.a. | | hypothetical protein | 521.1 | 414.6 | 355.22 | 430.3 |
| AG1IA_09643 | n.d. | n.a. | | hypothetical protein | 0 | 0 | 0 | 0 |
| AG1IA_09728 | 5 | n.a. | | hypothetical protein | 1.24 | 1.54 | 0.74 | 1.18 |
| AG1IA_09836 | n.a. | 18 hpi | | hypothetical protein | 47.64 | 41.95 | 36.13 | 41.91 |
| AG1IA_09837 | n.d. | 10 hpi | | hypothetical protein | 0 | 0 | 0 | 0 |
| AG1IA_09956 | 3 or 4 | n.a. | yes | hypothetical protein | 173.67 | 148.5 | 123.75 | 148.6 |
| AG1IA_10146 | 4 or 6 | n.a. | | hypothetical protein | 38 | 98.71 | 86.25 | 74.32 |
| AG1IA_10180 | n.a. | n.a. | | hypothetical protein | 2.23 | 2.63 | 3.06 | 2.64 |
| AG1IA_10284 | 1 | n.a. | | hypothetical protein | 0 | 0 | 0 | 0 |
| AG1IA_10296 | n.a. | 10 hpi | | hypothetical protein | 24.79 | 20.71 | 24.11 | 23.2 |
| AG1IA_10375 | n.a. | n.a. | | valine-tRNA ligase | 72.02 | 72.31 | 64.21 | 69.52 |
| AG1IA_10403 | n.a. | n.a. | | hypothetical protein | 9.1 | 8.83 | 12.65 | 10.19 |
| AG1IA_10405 | n.a. | 18, 24 hpi | yes | hypothetical protein | 0.4 | 0.45 | 0.81 | 0.55 |
| AG1IA_10478 | 5 | n.a. | | hypothetical protein | 12.03 | 14.08 | 17.09 | 14.4 |

^a Cluster numbers categorized with their expression profiles during infection on *Brachypodium distachyon* in this study as shown in Figure 5.

^b Expression timing (hours) after inoculation on rice plants determined by Zheng et al. (2013).

^c Annotations were obtained from top hit of blastP search.

^d FPKM (fragments per kilobase of exon per million reads mapped) of 3 independent RNA-seq analysis using total RNA prepared from growing hyphae of *R. solani*.

Transient expression of *RsSEPGs* expressed in the necrotrophic stage of infection

The *RsSEPGs* expressed at a later infection stage are expected to be involved in the induction of necrosis. Direct injections of purified proteins of the candidate secreted proteins of *R. solani* into leaves were used to survey their necrosis inducing activity (Zheng *et al.* 2013). For this purpose, *Agrobacterium*-mediated transient expression system can be employed and a model plant *Nicotiana benthamiana* provides a useful experimental platform. To date, *AGLIP1* in *R. soani* AG-1 IA was shown to induce necrosis in *N. benthamiana* (Li *et al.* 2019). Similarly, transient expression of *NLPI* gene of *R. soani* AG-8 caused necrosis (Anderson *et al.* 2016). Recently, it was shown that *RsIA_NP8* of *R. solani* AG-1 IA induced cell death when it was agroinfiltrated into *N. benthamiana* leaves and this phenotype was canceled by the silencing of SGT1 and HSP90 (Wei *et al.* 2020). In this case, the results suggest that this cell death phenotype was a result of disease resistance response by the recognition of the expressed protein as an avirulent factor in the non-host plant.

In this study, 10 *RsSEPGs* which were expressed mainly in the later stage of the infection (Table 8) were selected for further functional evaluation experiments for their necrosis induction activity using *N. benthamiana*. Each *RsSEPG* was sub-cloned into a pGWB2 vector to express them driven by the CMV 35S promoter and they were transformed into two *Agrobacterium* strains GVA3101 and EHA101. Among the infiltrated genes, three of them (*AG1IA_02940*, *AG1IA_08487*, and *AG1IA_07047*) expressed in *N. benthamiana* leaves were able to trigger necrotic lesions with variable degrees compared to the empty vector (Figure 8). These results may reflect their potential roles in the pathogenicity of *R. solani*. I also infiltrated the *Agrobacterium* cells transformed with *RsSEPGs* into *B. distachyon* leaves but the phenotypes were not clear.

Table 8. Primers used for plasmid construction for transient expression of *RsSEPGs* expressed in the necrotrophic stage of *R. solani* infection.

| Gene ID | Fw. Primer | Rv. primer |
|-------------|--------------------------|-----------------------------|
| AG1IA_09060 | CACCATGGTCAAGTCTGCTG | TCAGTAGATGGTCGTATTATCATTGGG |
| AG1IA_06739 | CACCATGCTCCTCCGTCTG | TTACGTTGTGGAGCGGTCTC |
| AG1IA_05783 | CACCATGCTTTTTAAACCCCTC | TCACAAGTTATTGGTCGAAGTC |
| AG1IA_09728 | CACCATGATTTGGGCACTGAC | CTAAGCGTTGAATCGCTTAAAAG |
| AG1IA_03254 | CACCATGACAATATCCACTTGG | TCACAGTCCATAGGTTCAAATAG |
| AG1IA_00273 | CACCATGAAATTCGTCAGCTTTG | CTAAGCTTGAACATCTCCAGTG |
| AG1IA_04819 | CACCATGCATCCATATTTG | TCAGTATCGTCCCAGAATTGG |
| AG1IA_07075 | CACCATGCGCTCCTTTGGAC | TCAACAAGGAAAAGAAAGTAAAGTG |
| AG1IA_06710 | CACCATGAGCCTGATGTTAC | TTATCCCAAGCTCTCTCAAGC |
| AG1IA_02940 | CACCATGCGGTTCATCTTTC | CTATCCACAGATCCAACCC |
| AG1IA_08487 | CACCATGTACACCCTCCTTCAAAC | CTAGCGCCGTAGTGAGTAATAAC |
| AG1IA_08777 | CACCATGTTCTTCAACTTTGCTTC | TCACTTTCCTCCTGATTCCTTGG |
| AG1IA_07047 | CACCATGATCGTCGTCCTCG | CTAGCCATGACTGCACGGG |

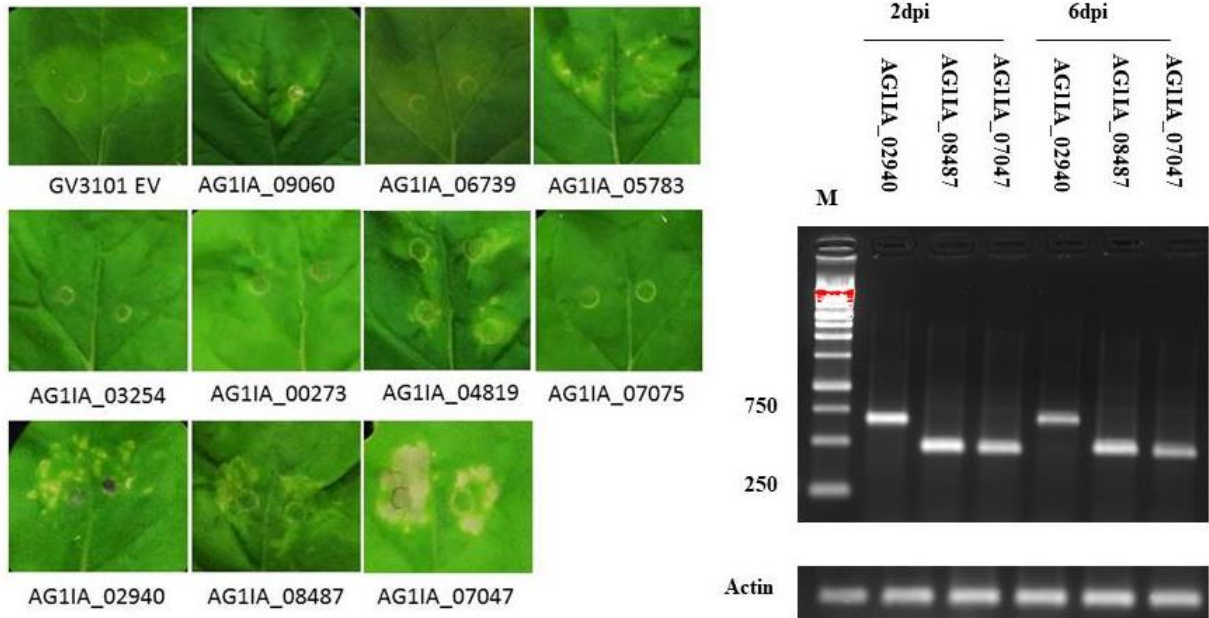


Figure 11. Transient expressions of 10 *RsSEPGs* by the Agro-infiltration method in *Nicotiana benthamiana*. Three genes *AG1IA_02940*, *AG1IA_0848*, and *AG1IA_07047* induced a variable degree of cell death symptoms in *N. benthamiana* (Left panel); their expression was detected semi-quantitatively by RT-PCR at 2 and 6 dpi using the actin gene as an internal control (Right panel). Representative photographs were taken 7-day post-infiltration. GV3101EV, *N. benthamiana* leaves infiltrated with *A. tumefaciens* strain GV3101 harboring pGWB2 binary vector.

Discussion

Transcriptome analysis during infection is used for the identification of the differentially expressed genes involved in pathogenicity. However, the detection of pathogen-derived transcripts using dual RNA-seq is technically problematic, especially at the early infection stage due to a small amount of pathogen's biomass in the sample and lack of synchronous fungal growth. Several ingenious methods for detection or sampling have been reported so far to overcome this issue (Asai *et al.* 2014, Nobori *et al.* 2018). To avoid these obstacles, the newly developed inoculation method was used in this study for the analysis of expression of the identified *RsSEPGs* during infection. Briefly, the number of inocula in a particular leaf area was increased. Also, a sheet was inserted between the inoculant and leaves to increase the synchronicity of the infection stage. qRT-PCR was used for the detection of transcripts to expect higher sensitivity.

By using the improved infection method, the transcripts of 52 *RsSEPGs* could be detected in at least one infection time point during the time course (6 to 32) and their expression patterns could be characterized. Among them, the expressions of 22 and 18 genes were also detected in the previously reported dual-transcriptome analyses during infection of *R. solani* on rice by Zheng *et al.*, 2013 and Xia *et al.*, 2017, respectively (Table 7). This means that *R. solani* should use a similar set of genes for the infection in the different hosts. In this study, 22 genes were newly detected, suggesting that the improved inoculation method may function well for the detection of *R. solani* RNAs *in planta*. In addition, the expression timing of each gene could be provided with a certain resolution and it would be helpful to speculate their virulence function. In this study, 6 *RsSEPGs* were detected with varied expression patterns in two independent experiments. The expression of these genes may be more sensitive to some environmental factors rather than infection progression.

Among the initially predicted 88 *RsSEPGs*, transcription of 68 genes was detected in our RNA-seq analysis and 57 genes (64.8%) need to be calibrated in their annotated gene model. Accurate annotation of secreted small proteins seems to be difficult. The candidate selection step using *de novo* assembled cDNAs based on RNA-seq data as performed by Yamamoto *et al.* 2019 will provide additional potential genes to be evaluated as an effector.

The expression patterns of the 52 *RsSEPGs* during the infection were classified into 6 clusters and the clusters 1–3 include 23 genes with their peaks of expression level at 6–16 hpi. While the remaining 29 genes categorized as clusters 4–6 were expressed mainly at 24–32hpi. These expression timing would be related to their function in pathogenicity. The *RsSEPGs*

expressed at the early infection stage are expected to have roles for suppression of host immunity.

Besides, *RsSEPGs* expressed at the later infection stage are expected to be involved in the induction of necrosis. Functional analysis of these *RsSEPGs* can open new avenues towards the understanding of the molecular pathogenicity of *R. solani*. However, gene knockout analysis is unavailable in *R. solani*. As alternative approaches, ectopic expression in plant cells, heterologous expression using bacterial pathogen, and identification of interactors from host plants can be employed. In this study, I used a transient expression system. Transient expression of 10 genes expressed in the later stage of infection showed that 3 genes in cluster 6 (*AG1IA_02940*, *AG1IA_08487*, and *AG1IA_07047*) could trigger cell death when they agroinfiltrated into *N. benthamiana* leaves (Figure 8). Further investigations for the mechanism underlying the cell death phenotype are required to confirm their virulence function because they did not reproduce such necrotic lesions in *B. distachyon*.

To speculate its virulence functions, sequence similarity to known proteins or domains are also useful. Among 61 *RsSEPGs*, 19 genes were given protein annotations or conserved domains with blastP and pfam search (Table 7). Four *RsSEPGs* in the cluster 1–3 showed similarity to proteins with known functions. *AG1IA_06325* has an identity (82.6%) with FK506 binding protein peptidylprolyl isomerase (a cyclophilin) which belongs to immunophilins family (Singh 2018). Cyclophilins are conserved protein families in animals, plants, fungi, oomycetes, and so on, and they are reported to be involved in diverse biological processes. Their functions in pathogenicity were also demonstrated in *Magnaporthe oryzae*, *Botrytis cinerea*, *Cryphonectria parasitica*, and *Puccinia triticina* (Viaud *et al.* 2002, Panwar *et al.* 2013). *Phellinus sulphurascens*, a basidiomycetes pathogen same as *R. solani*, highly induced a cyclophilin gene during the early stage of root colonization on conifer (Williams *et al.* 2014). Because cyclophilins are involved in plant immunity, loading of pathogen's cyclophilins into host cells may disturb defense response.

The amino acid sequences of *AG1IA_08487* and *AG1IA_08488* exhibit homology to ribonuclease (RNase)-containing proteins. In our experiment, *AG1IA_08487* could induce mild necrosis in the infiltrated leaves of *N. benthamiana*. Similarly, RNase-like effectors in *Blumeria graminis* was recently found to induce disease susceptibility in wheat and *N. benthamiana* when it was expressed in the host plants. This effector is thought to be a pseudoenzyme and inhibits methyl jasmonate-triggered degradation of host ribosomal RNA leading to cell death through interaction with host RNases (Pennington *et al.* 2019). This action may contribute to the suppression of host immunity. In our experimental system, *AG1IA_08488*

was shown to be expressed at the early infection stage (6 and 10 hpi). Its encoding protein may be a pseudoenzyme with a similar virulence function. On the contrary, *AG1IA_08487* was detected in the later infection stage such as clusters 3 or 6. This may retain RNase activity and degrade host RNAs to facilitate necrotrophic invasion.

An avirulent (AVR) effector AVR-Pita of *M. oryzae* encodes a putative neural zinc metalloprotease and it accumulates in a particular surface area of infection hyphae which is called biotrophic interfacial complex (BIC) (Zhang and Xu 2014). Although its virulence function has not yet been demonstrated, it is recognized by a disease resistance protein Pi-ta in rice, suggesting its function in pathogenicity (Jia *et al.* 2000). Because *AG1IA_00951* in cluster 6 shows similarity to metalloprotease, it might play a certain role in the formation of sheath blight necrotrophic lesions on *B. distachyon*.

Carbohydrate-binding proteins act as hydrolase enzymes for plant cell wall components and have a significant role in pathogenicity (Lombard *et al.* 2014). Many of the carbohydrate-active enzymes encoded by *R. solani* genome are expressed during infection on rice (Zheng *et al.* 2013, Xia *et al.* 2017). In the *RsSEPGs*, *AG1IA_00669* and *AG1A_04819* were identified as genes encoding carbohydrate-binding domain-containing proteins. Given that they satisfy criteria for secretory effector, they may have specific virulence functions such as masking of microbe-associated molecular patterns as found in Lysin motifs (LysM)-domain containing proteins (Bolton *et al.* 2008, Dörfors *et al.* 2019).

AG1IA_09055 and *AG1IA_09060* in the clusters 5 and 4, respectively, share homology with a thaumatin-like protein. This protein was identified as a secretory protein in *R. solani* AG-8. One thaumatin gene (*RsAG8_08836*) was significantly up-regulated in infected root tissue at 2 days post-infection and transient expression of this gene with agroinfiltration in *N. benthamiana* induced necrosis (Anderson *et al.* 2016). These thaumatin-like protein genes probably have a role in necrotrophic interaction.

It was previously shown that the *B. distachyon* accessions Bd3-1, Gaz-4, and Tek-4 are resistant to *R. solani* AG-1 IA (Kouzai *et al.* 2018a, Kouzai *et al.* 2016, Kouzai *et al.* 2020). This *R. solani*-*B. distachyon* relationship would rely on the incompatible interaction because they triggered the SA-dependent defense responses. The *RsSEPGs* identified in this study may contain avirulent factors that are recognized by *R. solani*.

References

- Agrios, G. Plant pathology: Fifth edition. Plant Pathology: Fifth Edition (2004).
- Anderson, J.P. *et al.* Proteomic analysis of *Rhizoctonia solani* identifies infection-specific, redox associated proteins and insight into adaptation to different plant hosts. Mol. Cell. Proteomics 15, 1188–1203 (2016).
- Asai, S. *et al.* Expression profiling during Arabidopsis/downy mildew interaction reveals a highly-expressed effector that attenuates responses to salicylic acid. PLoS Pathog. 10, e1004443 (2014).
- Cheng, S. F. *et al.* Ser/Thr kinase-like protein of *Nicotiana benthamiana* is involved in the cell-to-cell movement of *Bamboo mosaic virus*. PLoS One 8, e62907 (2013).
- De Jonge, R., Bolton, M.D. & Thomma, B.P.H.J. How filamentous pathogens co-opt plants: The ins and outs of fungal effectors. Curr. Opin. Plant Biol. 14, 400–406 (2011).
- Dörfors, F., Holmquist, L., Dixelius, C. & Tzelepis, G.A. LysM effector protein from the basidiomycete *Rhizoctonia solani* contributes to virulence through suppression of chitin-triggered immunity. Mol. Genet. Genomics 294, 1211–1218 (2019).
- Glazebrook, J. Contrasting mechanisms of defense against biotrophic and necrotrophic pathogens. Annu. Rev. Phytopathol. 43, 205–227 (2005).
- Irieda, H. *et al.* Conserved fungal effector suppresses PAMP-triggered immunity by targeting plant immune kinases. Proc. Natl. Acad. Sci. U. S. A. 116, 496–505 (2019).
- Jia, Y., McAdams, S.A., Bryan, G.T., Hershey, H.P. & Valent, B. Direct interaction of resistance gene and avirulence gene products confers rice blast resistance. EMBO J. 19, 4004–4014 (2000).
- Kawchuk, L.M. *et al.* Tomato *Ve* disease resistance genes encode cell surface-like receptors. Proc. Natl. Acad. Sci. U. S. A. 98, 6511–6515 (2001).
- Kim D., Pertea G., Trapnell C., Pimentel H., Kelley R. & Salzberg, S.L. TopHat2: accurate alignment of transcriptomes in the presence of insertions, deletions and gene fusions. Genome Biol. 14, R36 (2013).
- Kouzai, Y. *et al.* Expression profiling of marker genes responsive to the defence-associated phytohormones salicylic acid, jasmonic acid and ethylene in *Brachypodium distachyon*. BMC Plant Biol. 16, 59 (2016).
- Kouzai, Y. *et al.* Salicylic acid-dependent immunity contributes to resistance against *Rhizoctonia solani*, a necrotrophic fungal agent of sheath blight, in rice and *Brachypodium distachyon*. New Phytol. 217, 771–783 (2018a).
- Kouzai, Y. *et al.* Benzothiadiazole, a plant defense inducer, negatively regulates sheath blight resistance in *Brachypodium distachyon*. Sci. Rep. 8, 17358 (2018b).

- Kouzai, Y., Inoue, K., Uehara-Yamaguchi, Y., Takahagi, K., Nakayama, R., Matsuura, T., Mori, I.C., Hirayama, T., Abdelsalam, S.S.H., Noutoshi, Y. & Mochida, K. BdWRKY38 is required for the incompatible interaction of *Brachypodium distachyon* with the necrotrophic fungus *Rhizoctonia solani*. *Plant J.* Accepted article (2020) DOI: 10.1111/tpj.14976
- Li, S. *et al.* The effector AGLIP1 in *Rhizoctonia solani* AG1 IA triggers cell death in plants and promotes disease development through inhibiting PAMP-triggered immunity in *Arabidopsis thaliana*. *Front. Microbiol.* 10, 2228 (2019).
- Lombard, V., Ramulu, H.G, Drula, E., Coutinho, P.M. & Henrissat, B. The carbohydrate-active enzymes database (CAZy) in 2013. *Nucleic Acids Res.* 42, 490–495 (2014).
- Lorang, J.M., Sweat, T.A. & Wolpert, T.J. Plant disease susceptibility conferred by a ‘resistance’ gene. *Proc. Natl. Acad. Sci. U. S. A.* 104, 14861–14866 (2007).
- Nobori, T. *et al.* Transcriptome landscape of a bacterial pathogen under plant immunity. *Proc. Natl. Acad. Sci. U. S. A.* 115, E3055–E3064 (2018).
- Nováková, M., Šásek, V., Dobrev, P.I., Valentová, O. & Burketová, L. Plant hormones in defense response of *Brassica napus* to *Sclerotinia sclerotiorum* - Reassessing the role of salicylic acid in the interaction with a necrotroph. *Plant Physiol. Biochem.* 80, 308–317 (2014).
- Panwar, V., McCallum, B. & Bakkeren, G. Host-induced gene silencing of wheat leaf rust fungus *Puccinia triticina* pathogenicity genes mediated by the *Barley stripe mosaic virus*. *Plant Mol. Biol.* 81, 595–608 (2013).
- Pennington, H.G. *et al.* The fungal ribonuclease-like effector protein CSEP0064/BEC1054 represses plant immunity and interferes with degradation of host ribosomal RNA. *PLoS Pathog.* 15, e1007620 (2019).
- Saeed, A.I. *et al.* TM4 microarray software suite. *Methods Enzymol.* 411, 134–193 (2006).
- Selin, C., de Kievit, T.R., Belmonte, M. F., Fernando, W.G.D. & Monaghan, J. Elucidating the role of effectors in plant-fungal interactions: Progress and challenges. *Front. Microbiol.* 7, 600 (2016).
- Shang, S. *et al.* A novel effector CfEC92 of *Colletotrichum fructicola* contributes to glomerella leaf spot virulence by suppressing plant defences at the early infection phase. *Mol. Plant Pathol.* 21, 936–950 (2020).
- Singh, K., Winter, M., Zouhar, M. & Ryšánek, P. Cyclophilins: less studied proteins with critical roles in pathogenesis. *Phytopathology* 108, 6–14 (2018).
- Tan, K., Oliver, R.P., Solomon, P.S., & Moffat, C.S. Proteinaceous necrotrophic effectors in fungal virulence. *Funct. Plant Biol.* 37, 907–912 (2010).

- Toruño, T.Y., Stergiopoulos, I., & Coaker, G. Plant-pathogen effectors: Cellular probes interfering with plant defenses in spatial and temporal manners. *Annu. Rev. Genet.* 54, 419–441 (2016).
- Untergasser, A. *et al.* Primer3-new capabilities and interfaces. *Nucleic Acids Res.* 40, e115 (2012).
- Viaud, M.C., Balhadère, P.V & Talbot, N.J.A *Magnaporthe grisea* cyclophilin acts as a virulence determinant during plant infection. *Plant Cell* 14, 917–930 (2002).
- Vincent, D., Rafiqi, M. & Job, D. The multiple facets of plant–fungal interactions revealed through plant and fungal secretomics. *Front. Plant Sci.* 10, 1626 (2020).
- Wang, X. *et al.* The role of effectors and host immunity in plant – necrotrophic fungal interactions. *Virulence* 5, 722-732 (2014).
- Williams, H.L. *et al.* Gene expression profiling of candidate virulence factors in the laminated root rot pathogen *Phellinus sulphurascens*. *BMC Genomics* 15, 603 (2014).
- Witzel, K. *et al.* Recent progress in the use of ‘omics technologies in brassicaceous vegetables. *Front. Plant Sci.* 6, 244 (2015).
- Xia, Y. *et al.* Transcriptome analysis reveals the host selection fitness mechanisms of the *Rhizoctonia solani* AG1IA pathogen. *Sci. Rep.* 7, 10120 (2017).
- Yamamoto, N. *et al.* Integrative transcriptome analysis discloses the molecular basis of a heterogeneous fungal phytopathogen complex, *Rhizoctonia solani* AG-1 subgroups. *Sci. Rep.* 9, 19626 (2019).
- Zheng, A. *et al.* The evolution and pathogenic mechanisms of the rice sheath blight pathogen. *Nat. Commun.* 4, 1424 (2013).

Appendices

Appendix A: Preparation of plasmid for transient expression of *RsSEPGs* using Gateway® cloning.

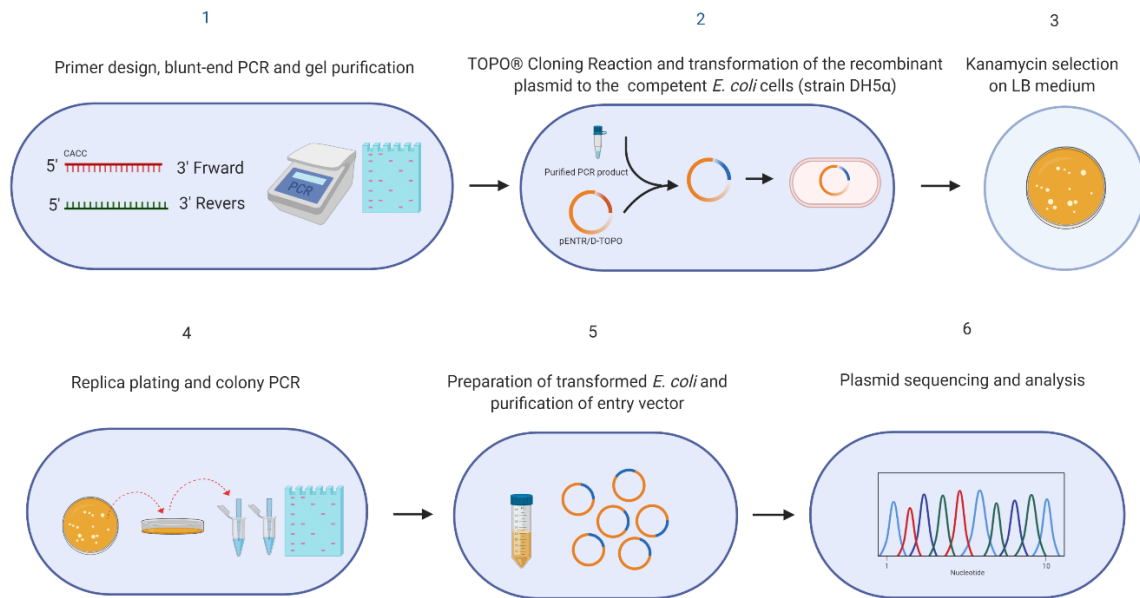


Figure A.1) preparation of the entry vector using TOPO cloning reaction. 1) Blunt-end PCR for the ORF of *RsSEPGs* was amplified from the cDNA generated from RNA extracted from *Brachypodium distachyon* leaves at 24hpi by *Rhizoctonia solani*. PCR products were verified by gel electrophoresis; the bands with the potential size were gel purified using FastGene® Gel/PCR Extraction Kits (NIPPON GENETICS, CO., Ltd) 2). The purified PCR products were TOPO cloned to the pENTR™/D-TOPO® vector using pENTR™ Directional TOPO® Cloning Kits (Invitrogen). The recombinant pENTR™/D-TOPO® vector was transformed to One Shot® Competent *E. coli* (Strain DH5α™) using a heat shock. 3) Transformed *E. coli* were cultured on LBA medium supplemented with Kanamycine sulfate 50µg/ml. 4) Positive colonies were verified for the correct insert using colony PCR. 5,6) Preparation of the entry vector (using FastGene® Plasmid Mini Kit (Nippon Genetics Co., Ltd)) and sequence verification.

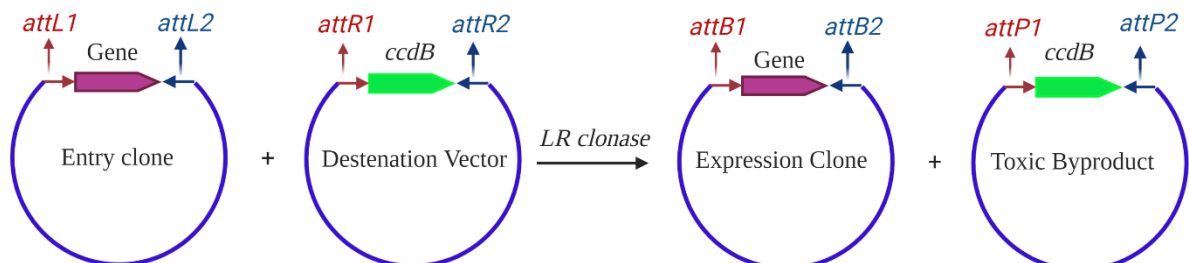


Figure A. 2) Preparation of the destination vector; Gateway® LR Clonase® II enzyme mix was used to transfer the gene of interest (*RsSEPGs*) from the entry clones to the Gateway Binary vector (pGWB2). The destination vector (pGWB2) was then transformed into an electrocompetent *Agrobacterium tumefaciens* strain GV3101. Which was selected using an LBA supplemented with Hygromycine B and Knamycine sulfate (50µg/ml). Positive colones were verified by colony PCR to check the potential size of the insert.

Appendix B: Transient expression procedure using Agro-infiltration method

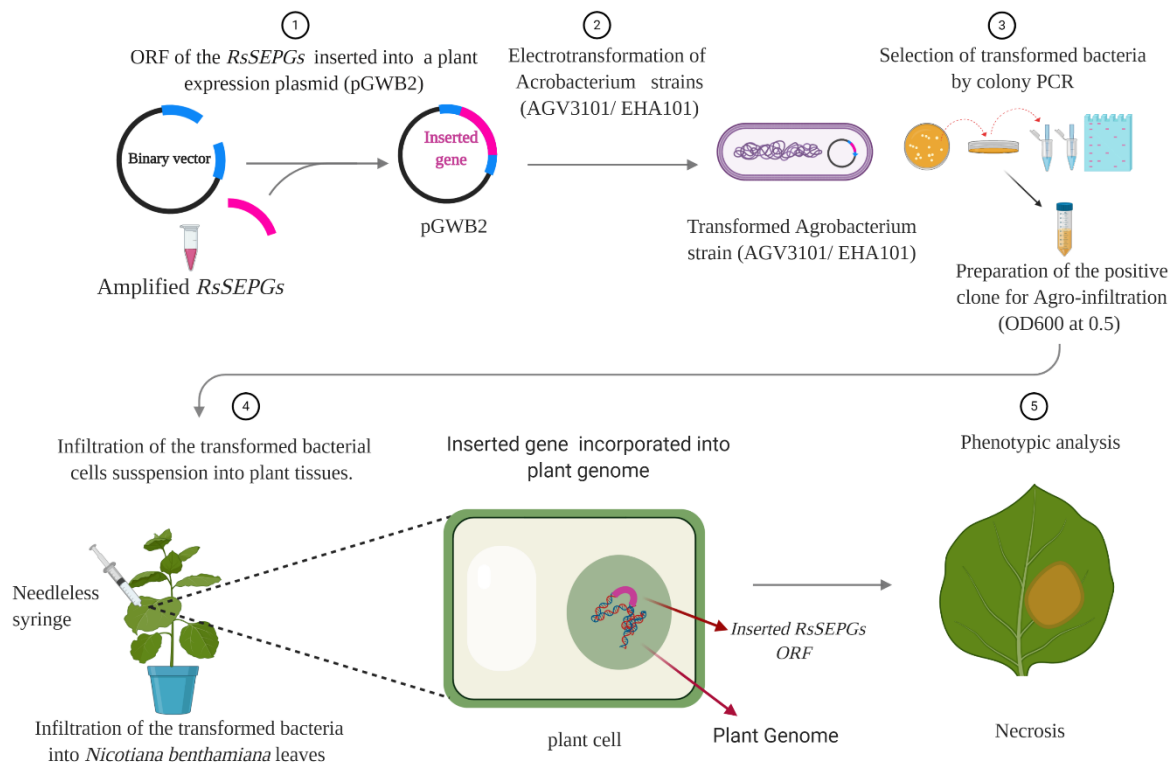


Figure B.1) General workflow of the transient expression using agroinfiltration of *Nicotiana benthamiana*. 1) The gene of interest (*R_sSEPGs*) was shuttled into a Gateway Binary vector (pGWB2) *Via* LR reaction to prepare the expression vector with the gene of interest. 2) The expression plasmid (pGWB2) electrotransformed to the electrocompetent *Agrobacterium tumefaciens* strain GV3101. 3) Colonies with the correct insert size were selected by colony PCR; subsequently positive colonies were prepared in an infiltration solution (10 mM MES pH = 5.6, 10 mM MgCl₂, 0.03% Tween20, 200 μM acetosyringone) for Agro-infiltration. 4) a needleless syringe was used to infiltrate the *A. tumefaciens* suspension into the leaves of *N. benthamiana* at four weeks of age. 5) The infiltrated leaves were checked daily for necrosis induction; the leaves were collected and photographed at seven-day post infiltration.